Journal of Petroleum Science and Engineering 210 (2022) 110057

Contents lists available at ScienceDirect

Journal of Petroleum Science and Engineering

journal homepage: www.elsevier.com/locate/petrol

Geochemistry of formation waters and crude oils in the Shulu Sag, Bohai Bay Basin, NE-China, to assess quality and accumulation of hydrocarbons

Chuan Cai [a,b], Nansheng Qiu [a,b,*], Nian Liu [a,b], Zhenming Li [c], Yuanjie Wang [d], Zhanwen Yu [d], Ting Gao [d], Yaxian Jiao [d]

[a] State Key Laboratory of Petroleum Resource and Prospecting, China University of Petroleum, Beijing 102249, China
[b] College of Geosciences, China University of Petroleum, Beijing 102249, China
[c] Wuxi Research Institute of Petroleum Geology, Sinopec Exploration and Production Research Institute, Wuxi 214126, Jiangsu, China
[d] PetroChina Huabei Oilfield Company, Renqiu, Hebei 062552, China

ARTICLE INFO

Keywords:
Formation water
Biodegradation
Water washing
Hydrocarbon preservation
Buried hills
Shulu sag

ABSTRACT

Geochemical fingerprinting of formation waters and hydrocarbons can be utilized to track the migration, accumulation, and preservation of hydrocarbons. The present case study from the Shulu Sag, Bohai Bay Basin, NE-China analyzes the origin of the formation waters and the relationship between water chemistry and hydrocarbon preservation by combining the geochemical characteristics of formation waters and crude oils. There are three geochemical groups of formation waters with different origins, which represent different hydrodynamic environments and hydrocarbon preservation conditions. Group 1 waters are related to meteoric water with the lowest total dissolved solids (TDS), γ(Cl–Na)/γMg and the highest γNa/γCl, representing an open environment with poor hydrocarbon preservation conditions, accompanied by super heavy oils. Group 3 waters are connate water with the highest TDS, γ(Cl–Na)/γMg and the lowest γNa/γCl, representing a closed environment with the best hydrocarbon preservation conditions, accompanied by light oils. Group 2 waters are intermediate between Group 1 and Group 3 waters, representing a semi-open environment with intermediate hydrocarbon preservation conditions, accompanied by light, medium, and heavy oils. The clear corresponding relationship between oil quality and associated water type shows that water chemistry significantly affects the oil quality and accumulation in the Shulu Sag through secondary changes. Biodegradation is the dominant effect in the strata above 2100 m. Water washing is dominant in the depth range of 2100–3400 m, and there are no noticeable secondary changes in the strata below 3400 m. A model for the origin, evolution, and flow of formation waters in the Shulu Sag is established to analyze the hydrocarbon accumulation process. Meteoric waters flow into the buried hills from Ningjin Uplift as a result of gravity flow, resulting in modification of oil composition, destruction of the oil reservoirs, and the formation of Group 1 waters. During the hydrocarbon charging, the centrifugal flow driven by overpressure flows in two directions from the source rocks, one is to the western slope and mixes with meteoric waters to form Group 2 waters and heavy oil reservoirs, and the other is to the paleo-uplift to form Group 2 and Group 3 waters and light oil reservoirs. Water chemistry is sensitive to the hydrodynamic environment change and can be an important reference for oil and gas exploration. Buried hills with Group 3 waters should be the highest priority for further exploration, whose oil reservoirs are dominated by light oil with high commercial value. Although the oil quality is poor, buried hills with Group 2 waters in the slope can be secondary targets. In comparison, the buried hills with Group 1 waters should be avoided for oil and gas exploration. The geochemistry of formation waters helps understand the origin and evolution of formation waters, predict oil quality and distribution, and further aids oil and gas exploration.

1. Introduction

In petroliferous basins, formation waters are involved in the generation, migration, accumulation, preservation, and loss of hydrocarbons (Lewan, 1997; Grasby et al., 2012; Li and Zeng, 2017; Yu et al., 2020). The depositional environment controls the original chemical

* Corresponding author. State Key Laboratory of Petroleum Resource and Prospecting, China University of Petroleum, Beijing 102249, China.
E-mail address: qiunsh@cup.edu.cn (N. Qiu).

https://doi.org/10.1016/j.petrol.2021.110057
Received 7 August 2021; Received in revised form 4 December 2021; Accepted 14 December 2021
Available online 17 December 2021

compositions of formation waters (An et al., 2021), which can be secondarily changed by subaerial evaporation, water-rock interactions, and the mixing with exogenetic fluids (e.g., shallow meteoric water and deep hydrothermal fluid) (Birkle et al., 2009; Belkhiri et al., 2011; Chen et al., 2018; An et al., 2021). Therefore, the water chemistry can provide much hydrogeological information, such as basin evolution and hydrodynamic conditions (Worden et al., 1999; Xie et al., 2006; Michael and Bachu, 2002; Li, 2016), the origin and evolution of waters (Chen et al., 2018; Saller and Stueber, 2018; Li and Cai, 2017; Engle et al., 2020), hydrodynamic environments and hydrocarbon preservation conditions (Dickey et al., 1987; Li and Zeng, 2017; Al-Hajeri and Bowden, 2017; Yu et al., 2020), and water-rock interactions (Du et al., 2010; Lüders et al., 2010; Saller and Stueber, 2018; Cortes et al., 2016; An et al., 2021).

Based on the isotopes and ionic concentrations, formation waters in the sedimentary basin are of various types with different origins and evolutionary processes (Bozau et al., 2015; Saller and Stueber, 2018; Hermides et al., 2020). Those waters represent different hydrodynamic environments, either open, semi-open or closed (Li and Zeng, 2017; Dong et al., 2020; An et al., 2021). Therefore, water chemistry is widely used to evaluate hydrocarbon preservation conditions and predict the optimum location for hydrocarbon accumulation. For example, Grasby et al. (2012) believed that the biogenic methane might be distributed along basin margins because its generation is associated with the biodegradation caused by the inflow of meteoric water. Li and Zeng (2017) suggested that the hydrodynamic blocking and discharge areas, dominated by Na–Cl and Ca·Na–Cl waters, were suitable for migrating and accumulating hydrocarbons. Al-Hajeri and Bowden (2017) successfully assessed the formation sealing by analyzing the geochemistry of formation water. Yu et al. (2020) proposed effective hydrochemistry parameters by machine learning to predict favorable areas for hydrocarbon preservation.

The studies mentioned above only use static hydrogeochemistry unilaterally to speculate on the hydrocarbon preservation conditions. They ignored the response characteristics of hydrocarbons to water chemistry, which may lead to incorrect interpretation and prediction, as the relationship between hydrocarbons and formation water remains controversial. For example, biodegraded oils are generally associated with low salinity water (Bockmeulen et al., 1983), but they may also coexist with high salinity water in some cases (Dickey et al., 1987). Therefore, in addition to water chemistry, the geochemical characteristics of crude oil should also be considered to explain the relationship between water and oil jointly. Moreover, in most basins studied, formation water and crude oil are of a single type (Li and Cai, 2017; Yu et al., 2019, 2020), which may provide an incomplete explanation for the impact of water on hydrocarbon preservation. Poor conditions for hydrocarbon preservation may reduce oil quality, resulting in the coexistence of many types of crude oils, such as normal oil, biodegraded oil, and condensate (Head et al., 2003; Larter et al., 2006; Alkhafaji, 2021). Therefore, the relationship between water chemistry and oil quality needs to be further verified by studies of complex basins with various types of formation waters and crude oils.

The origin and dynamic evolution of the formation water have been the focus of attention (Belkhiri et al., 2011; Panno et al., 2013; Saller and Stueber, 2018; Engle et al., 2020; Yu et al., 2021), but only a few studies have linked them to the migration and accumulation of petroleum (Li and Cai, 2017; Chen et al., 2018). Chen et al. (2018) suggested that the evolution of formation water could constrain hydrocarbon charging events based on the relationship between three types of brines and hydrocarbons in the Tarim Basin. Moreover, the water flow can indicate hydrocarbon migration (Li and Cai, 2017) because hydrocarbons from the secondary migration are mostly driven by water flow (Tissot and Welte, 1984). More attention should be paid to the dynamic evolution of the formation water and its relationship to hydrocarbon accumulation besides static characteristics.

The Shulu Sag is one of the critical blocks of oil and gas exploration in the Jizhong Depression, Bohai Bay Basin, China. PetroChina Huabei Oilfield has succeeded in petroleum exploration in the wells JG21, JG22, JG23, and JG33 in recent years, but the subsequent drillings have failed one after another. Moreover, the oil quality ranges from light to super heavy. Previous studies suggested that the lacustrine marlstone in the lower part of Mbr 3 of the Eocene Shahejie Fm in the Shulu Sag is the primary source rock (Li et al., 2017) that can provide oils for the buried hill reservoirs. In addition, carbonate rocks dominate the buried hill reservoirs with good storage capacity (Cai et al., 2020; Xiang et al., 2021). Regional unconformity connects source rock and reservoir and provides pathways for hydrocarbon migration (Cai et al., 2020). The main factors of hydrocarbon accumulation in the study area are still unclear, which greatly restricts further hydrocarbon exploration. In particular, the formation waters in the buried hills are abnormally active during the oil production testing, and the maximum water production is 2501 m^3/d. Active formation water may greatly affect the migration, accumulation, and preservation of hydrocarbons. However, the study of formation waters in the study area has not been reported so far.

The buried hills in the Shulu Sag have various types of formation water and crude oil, which is a suitable object for studying water's effects on hydrocarbon preservation. The primary purposes of this study are to 1) describe the chemical composition of the formation waters to analyze the origin and evolution of different kinds of formation waters; 2) describe the physical and geochemical characteristics of crude oils to determine their quality and biodegradation level; 3) discuss the relationship between water chemistry and oil quality and the mechanism by which water affect oil quality; 4) built the evolution model of formation water and its relationship to hydrocarbon accumulation. Compared with other studies (Grasby et al., 2012; Li and Zeng, 2017; Yu et al., 2020), our study differs in that 1) in addition to analyzing the hydrochemistry characteristics of the formation water, the response characteristics of crude oil to water chemistry are considered to clarify the relationship between water chemistry and oil quality; 2) the evolution model of formation water is built to explain the process of hydrocarbon accumulation. We expect to fill the gaps in the study area by analyzing the hydrocarbon preservation conditions from water chemistry. The result can help understand the application of water chemistry in evaluating hydrocarbon preservation conditions and aid hydrocarbon exploration for similar basins.

2. Geological and hydrogeological framework

The Shulu Sag is located in the southern part of the Jizhong Depression, Bohai Bay Basin, NE-China (Fig. 1a). It is a NE-trending and eastward-dipping fault-depression basin, controlled by the Hengshui Fault in the north, the Leijiazhuang Fault in the south, the Xinhe Fault in the east (Fig. 1). The study area can be divided into Ningjin uplift, western slope, and eastern sag from west to east (Fig. 1b). The Taijiazhuang and Jingqiu Faults created two paleo-uplifts in the eastern sag, where the first oil reservoirs were discovered (Fig. 1b). The NE-SW trending early faults are the main component of the buried hill traps in the western slope (Fig. 1c; Huang et al., 2018). The fault displacement of the NE-SW trending fault controls the height of the trap and the size of oil reservoirs. The discovered oil reservoirs include wells JG33, JG6, and JG14-1 in the Northern Slope, wells JG21, JG22, and JG23 in the Southern Slope, and wells JG1 and JG2 in the Paleo-uplift (Fig. 1b). In addition, wells J7 and J34 in the Southern Slope also produced a small amount of super-heavy oil, but no commercial reservoirs were formed (Fig. 1b).

The Shulu Sag consists of the buried hill strata and Cenozoic strata (Fig. 1c; Fig. 2). The buried hill strata, including the Proterozoic-Archean (Pt–Ar) carbonate and metamorphic rocks, the Cambrian-Ordovician (O-Є) carbonate rocks, and the Permo-Carboniferous (C–P) coal-bearing mudstone and sandstone, are eastward-dipping due to the downthrow of the eastern boundary fault (Huang et al., 2018). As shown in the light purple area in Fig. 1c, the top of the buried hill is the main area where oil and gas accumulate. Because the buried hill strata are

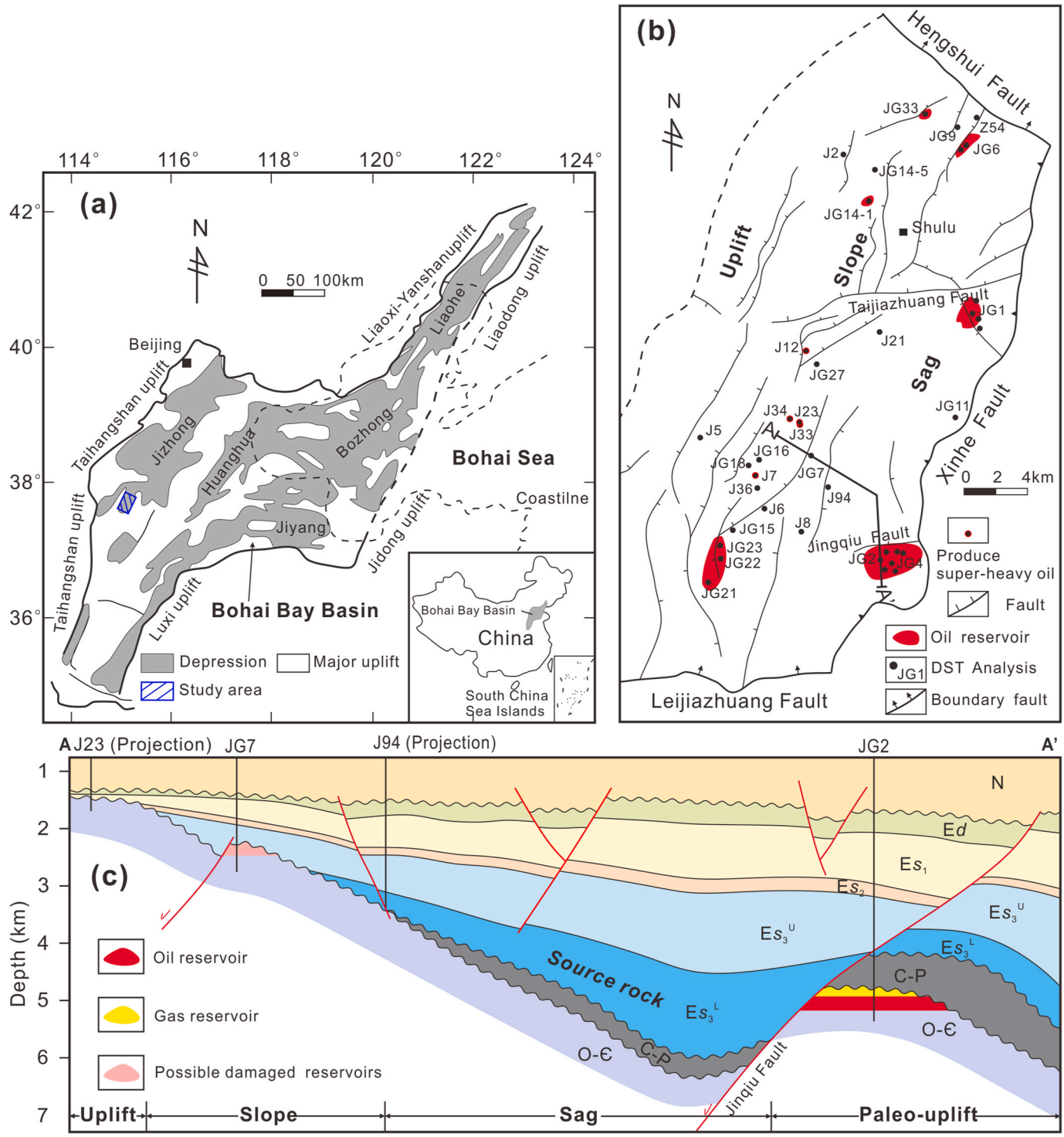

Fig. 1. (a) The location of the study area in the Bohai Bay Basin (Modified after Liu et al., 2017). (b) The structure of Shulu Sag and the locations of petroleum exploration well where drill-stem testing (DST) analysis is available (Modified after Cai et al., 2020). (c) Cross-section from uplift through the slope, sag to paleo-uplift showing simplified stratigraphy and tectonic belts. The detailed information of the strata is shown in Fig. 2.

inclined and eroded, the Proterozoic-Archean strata are only exposed in the Ningjin Uplift, and the Permo-Carboniferous strata are only preserved in the center of the sag (Fig. 1c; Xiang et al., 2021). Cambrian-Ordovician strata distributed in the Western Slope and Paleo-uplift are the main producing layer of oil and gas, which is dominated by calcite and dolomite, with 10–20% detrital minerals, such as quartz and feldspar, and clay minerals. The Cenozoic strata, which gradually overlap upward onto the buried hill strata, comprise five formations from bottom to top: the Shahejie (E*s*), Dongying (E*d*), Guantao (N*g*), Minghuazhen (N*m*), and Pingyuan (Q*p*) Fm (Fig. 1c; Fig. 2). The Shahejie Fm is composed of three members: Mbr 1 (Es_1), Mbr 2 (Es_2), and Mbr 3 (Es_3). Moreover, the Mbr 3 of the Shahejie Fm includes the lower (Es_3^L) and the upper part (Es_3^U).

The sedimentary environment and tectonic evolution jointly controlled the origin and evolution of the formation waters (Chen et al., 2018). Ordovician-Cambrian strata were deposited in the marine

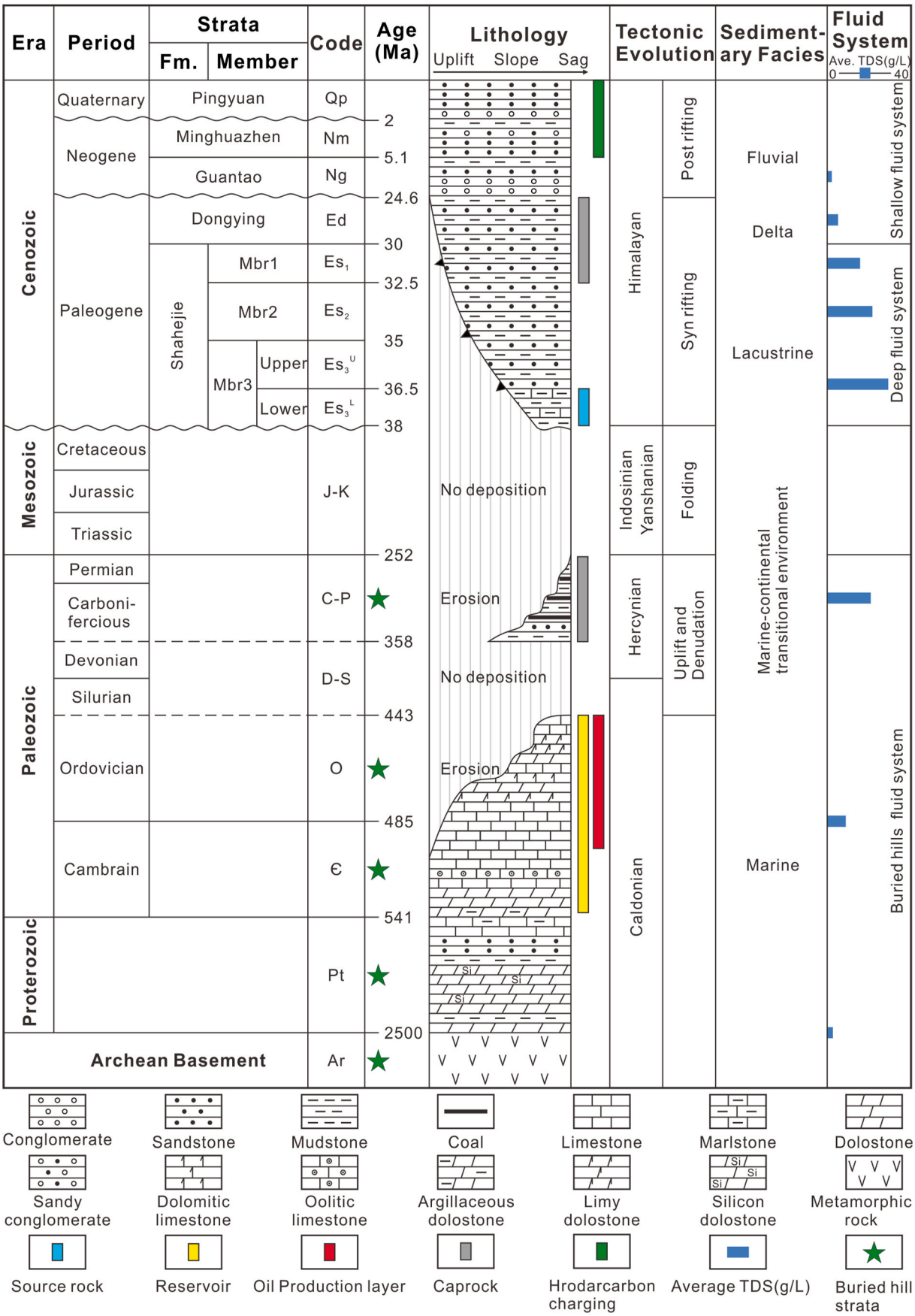

Fig. 2. Comprehensive stratigraphic column of the Shulu Sag (Modified after Xiang et al., 2021).

environment (Xiang et al., 2021). As a result of the Caledonian movement, the Ordovician-Cambrian strata were weathered and denuded from late Ordovician to Carboniferous (Fig. 2). After the deposition of the Permo-Carboniferous strata, the buried hill strata were again lifted and denuded by the Indosinian and Yanshanian movement until the Paleogene (Fig. 2; Xiang et al., 2021). As a result, the TDS of formation waters in the buried hill is lower than the Shahejie Fm (Fig. 2). Continuous lacustrine deposits developed in the early Paleogene, and gradually evolved into Neogene delta and fluvial deposits with the lake level decline (Fig. 2; Jiang et al., 2007). Consequently, the TDS of formation waters increase from Guantao to Mbr 3 of the Shahejie Fm (Fig. 2; Table S1 in the Supplementary Material). Based on the TDS and sedimentary environment, the Shulu Sag can be zoned as three fluid systems from top to bottom (Fig. 2): 1) Guantao-Dongying Fm shallow fluid system with low TDS formation waters (<5.00 g/L); 2) Shahejie Fm deep fluid system with the highest TDS formation waters; 3) buried hill fluid system in which formation waters have medium TDS due to the intrusion of meteoric water.

The buried hill fluid system is the focus of this study. Because the Xinhe boundary fault was intensively active in the early Paleogene, the eastern buried hills were buried along with the rapid deposition of the Mbr 3 of the Shahejie Fm (Jiang et al., 2007). In contrast, the western buried hills were buried relatively late and have been directly connected with the surface water system for an extended period of geological history, resulting in large-scale karst reservoirs (Cai et al., 2020; Xiang et al., 2021). It was not until the Guantao Fm deposition period that the western buried hills were entirely buried, leading to the weaker influence of meteoric water. Under different tectonic backgrounds, the formation water of the eastern and the western buried hills have undergone different evolutions.

3. Data and methods

In this study, 131 water data from 40 wells and 59 oil data from 27 wells in the buried hills were collected from PetroChina Huabei Oilfield, which were used to analyze the geochemical characteristics of formation waters and crude oils. These samples were taken from drill-stem testing (DST), and the analysis was performed at the Test Center of the Huabei Oilfield. The analysis results were recorded in the paper records of formation water analysis and crude oil analysis. Water samples were analyzed by ion-exchange chromatography for the major ions and cations (Na^+, Mg^{2+}, Ca^{2+}, Cl^-, SO_4^{2-} and HCO_3^-). Hitchon and Brulotte (1994) established a set of culling criteria to filter the water data based on chemical analysis. They have taken the Western Canadian Basin as an example to verify its effectiveness. According to these culling criteria, the sample will be rejected if the charge balance (cations-anions/cations + anions) is greater than 0.15. In addition, if the pH value is less than 5.0 or greater than 10.0, the sample should be removed as it is likely to be caused by water contamination. Please refer to Hitchon and Brulotte (1994) for more detailed culling criteria. In order to eliminate potential errors from drill-stem testing or data transcription, all formation water data were screened based on the method of Hitchon and Brulotte (1994). After culling, 98 water data from 34 wells were retained (Table S2 in the Supplementary Material), accounting for 75% of the original data, which are used to study the geochemistry of formation waters in the buried hills of the whole sag.

Oil data included physical parameters such as density, viscosity, sulphur content, wax content, solidification point, resin and asphaltene content (Table S3 in the Supplementary Material). In addition, oil samples from wells JG21, JG22, and JG33 were performed on the Gas chromatography-mass spectrometry (GC-MS) to determine maturity and biodegradation level. The oil samples cannot be obtained from wells JG1 and JG2 due to the long history, so the GC-MS data of JG1 oil was collected from PetroChina Huabei Oilfield. According to the standard experimental procedure, the GC-MS experiment was completed at the China University of Petroleum (Beijing).

4. Results

4.1. Water geochemistry

4.1.1. Total dissolved solids (TDS)

The TDS of modern seawater and formation waters from different formations is shown in Fig. 3a. The TDS of formation waters from the buried hills of Shulu Sag has a wide distribution range from 1.38 to 59.39 g/L and mainly distributes between 1.38 and 20.00 g/L (10.76 g/L on average). About 94% of the samples have lower TDS than modern seawater (Fig. 3a). The TDS of formation waters is segmented in the depth range of 938–5204 m (Fig. 3a). In the strata above 3400 m, the TDS is lower than 5.00 g/L, and the waters are mainly brackish. However, the TDS in the strata below 3400 m is generally greater than 5.00 g/L, and the waters are mainly saline with a small amount of brine.

As shown in Fig. 3b, the TDS of formation waters increase gradually from west to east. The Proterozoic-Archean Fm located on the Ningjin Uplift is the main window for meteoric water to flow into the buried hills, resulting in the lowest TDS (Fig. 3). The formation waters of the Cambrian-Ordovician Fm located on the Western Slope are mainly brackish. In contrast, the formation waters of the Cambrian-Ordovician Fm located on the Northern Slope and the Paleo-uplift are mainly saline. The formation waters of the Permo-Carboniferous Fm distributed in the Paleo-uplift have high salinity because they may be affected by the high salinity waters of the Shahejie Fm (Fig. 3).

4.1.2. Main ions characteristics

Fig. 4 shows the relative content of main ions of formation waters in the Piper and Radial diagram. Na^+ has the greatest concentration among the cations and ranges from 0.333 to 20.622 g/L (2.853 g/L on average). Ca^{2+} has a concentration from 0.025 to 15.150 g/L (0.899 g/L on average). The concentration of Mg^{2+} is the lowest, ranging from 0.006 to 1.847 g/L (0.140 g/L on average). The concentration of Ca^{2+} in some samples is greater than that of Na^+ (Fig. 4a). The major anions follow a concentration trend of $Cl^- > HCO_3^- > SO_4^{2-}$. The concentration of Cl^- ranges from 0.230 to 35.184 g/L (5.585 g/L on average). The concentration of HCO_3^- ranges from 0.201 to 7.628 g/L (0.878 g/L on average). The concentration of SO_4^{2-} ranges from 0.002 to 2.094 g/L (0.409 g/L on average). There is a linear relationship ($R^2 = 0.983$) between Cl^- concentration and the TDS (Fig. 5a). Although the correlations between Na^+, Ca^{2+}, and Mg^{2+} concentration and the TDS are poor, the Na^++Ca^{2+} has a positive correlation ($R^2 = 0.984$) with the TDS (Fig. 5b), indicating the TDS of formation waters is mainly controlled by the Cl^-, Na^+ and Ca^{2+}. Compared with modern seawater, the concentrations of Na^+, Mg^{2+}, Cl^- and SO_4^{2-} are lower, while HCO_3^- and Ca^{2+} are relatively enriched (Table S2 in the Supplementary Material).

4.2. Water type

In this study, formation waters were classified based on the relative content of anions and cations. As shown in Fig. 4a, formation waters from the buried hills in the Shulu Sag can be divided into three groups with different TDS, ion concentrations, and characteristic coefficients (Fig. 4; Fig. 6; Table 1). Two samples from wells JG22 and JG4 are special in the Piper diagram because of their high SO_4^{2-} and HCO_3^- concentration (Fig. 4a), but they still are classified into Group 2 because their major ions are Cl^- and Na^+, which is similar to the samples from wells JG23 and JG2 in Group 2.

Group 1 waters are Na–HCO_3·Cl waters with the lowest TDS (the average of 3.17 g/L) and primarily occur in the Ningjin Uplift and the Western Slope (Table 1). The water type of Sulin classification is $NaHCO_3$ (Table 1). The anion is mainly Cl^- with an average of 66.95% and contains many HCO_3^- with an average of 30.73%. The cation is mainly Na^+ with an average of 89.69%. In the Group 1 waters, the γNa/γCl varies from 1.09 to 1.68 with an average of 1.35, and the γ(Cl–Na)/γMg varies from −22.20 to −1.61 with an average of −9.82, the 100 ×

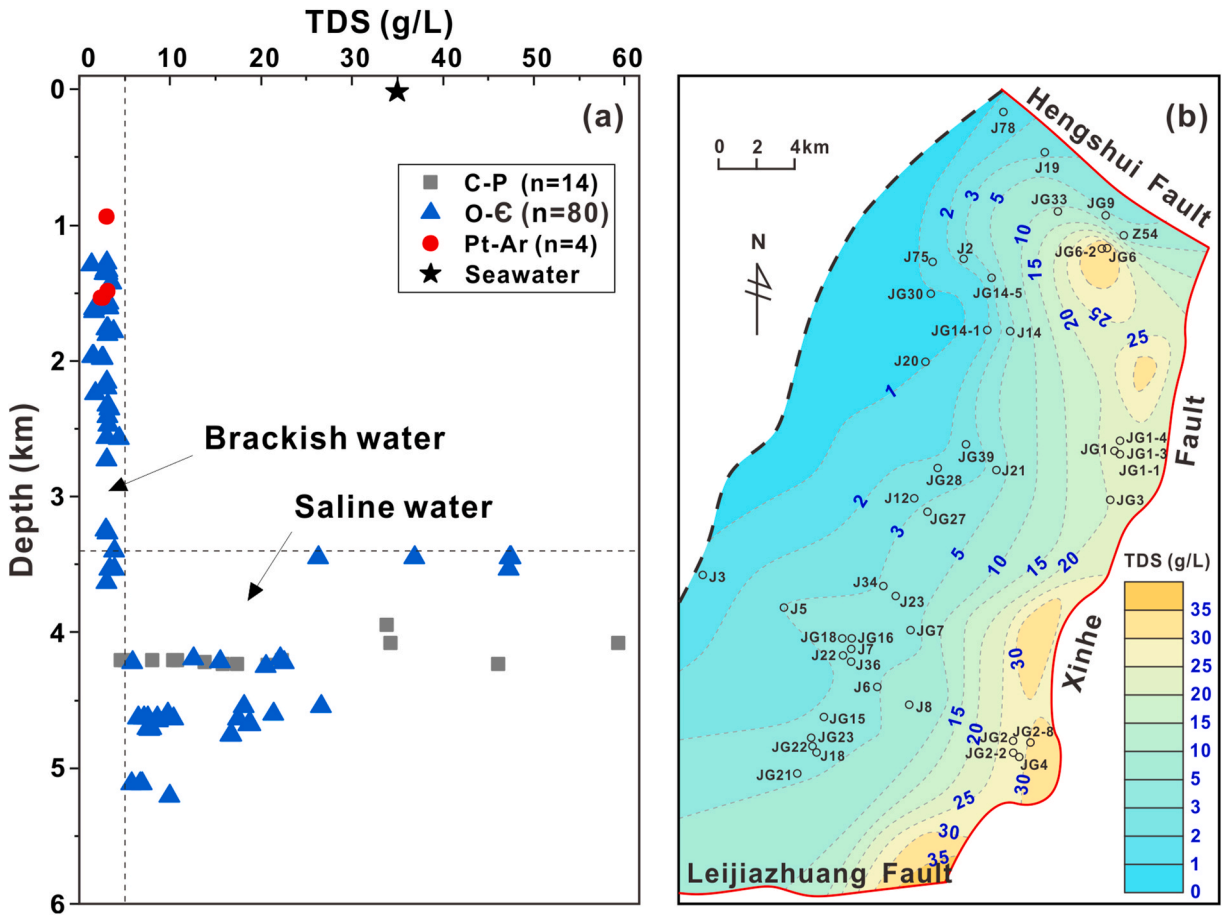

Fig. 3. (a) The scatter plots of TDS with depth. (b) Contour map showing the TDS of formation waters in the top of buried hills gradually increase from west to east.

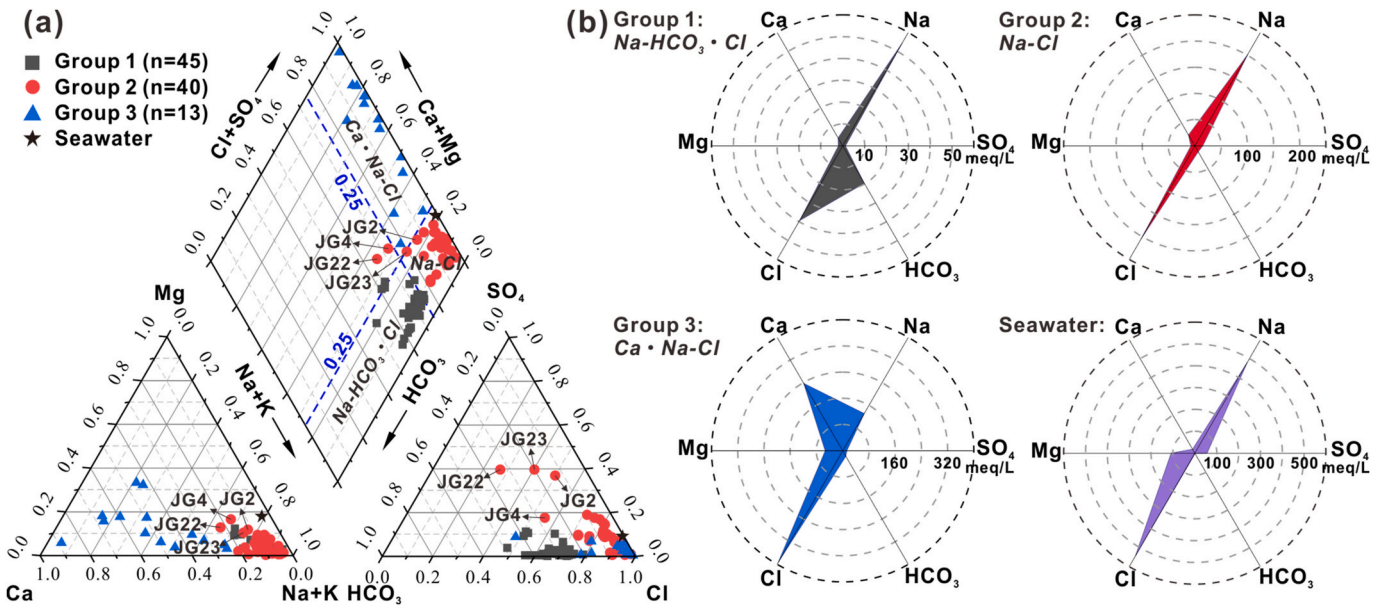

Fig. 4. Piper (a) and Radial (b) diagram showing relative content for main ions of formation waters from the buried hills in the Shulu Sag. (a) Three geochemical groups of formation water in the Shulu Sag were identified based on the relative content of anions and cations. (b) The chemical composition of formation waters differs from modern seawater, indicating that they have undergone different evolutions.

$\gamma SO_4/\gamma Cl$ varies from 0.12 to 21.83 with an average of 3.79 (Fig. 6; Table 1).

Group 2 waters are Na–Cl waters with higher TDS (the average of 14.61 g/L) and primarily occur in the Paleo-uplift and the Southern Slope (Table 1). Group 2 waters mainly include three types of water for Sulin classification: Na_2SO_4, $CaCl_2$, and $NaHCO_3$ (Table 1). The anion is

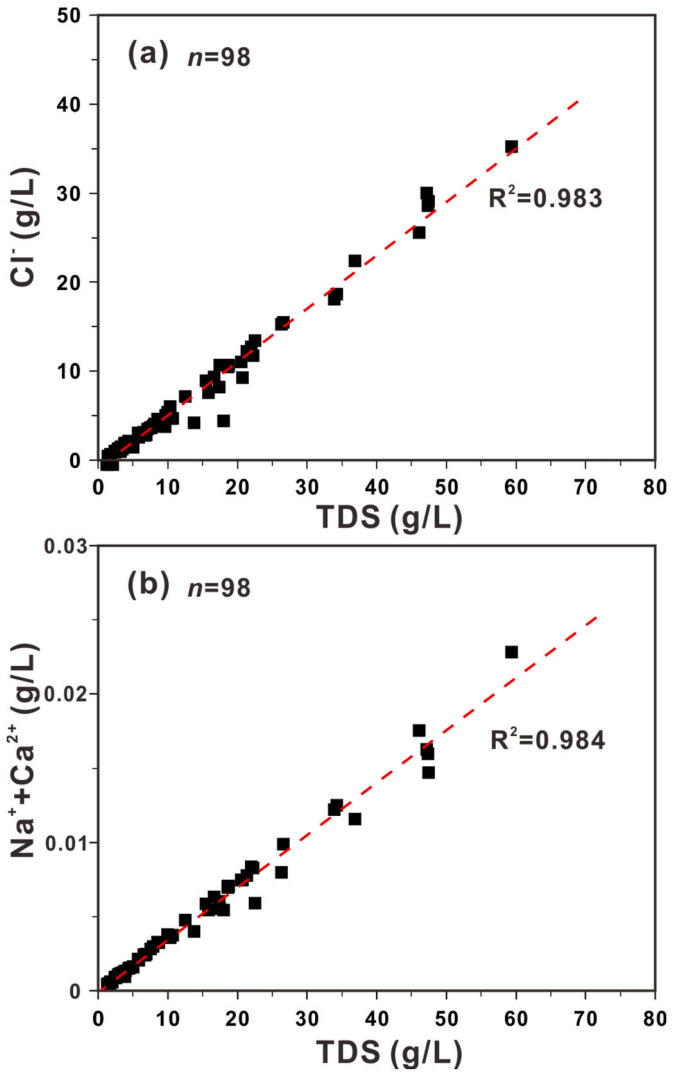

Fig. 5. The scatter plots of TDS vs. (a) Cl-, (b) Na^{+}+Ca^{2+} of formation waters from the buried hills of the Shulu Sag.

mainly Cl^{-} with an average of 81.87%, and the cation is mainly Na^{+} with an average of 86.23%. In the Group 2 waters, the γNa/γCl varies from 0.83 to 2.42 with an average of 1.10, and the γ(Cl–Na)/γMg varies from −23.67 to 12.15 with an average of −2.38, the 100 × $\gamma SO_4/\gamma Cl$ varies from 0.55 to 31.94 with an average of 9.92 (Fig. 6; Table 1). Some samples have a higher concentration of SO_4^{2-} and HCO_3^{-}, leading to a higher γNa/γCl and 100 × $\gamma SO_4/\gamma Cl$ (Fig. 4; Fig. 6).

Group 3 waters are Ca·Na–Cl waters with the highest TDS (the average of 24.21 g/L) and mainly occur in the Paleo-uplift and Northern Slope (Table 1). The water type of Sulin classification is $CaCl_2$ (Table 1). The anion is mainly Cl^{-} with an average of 90.99%, and the cation is mainly Ca^{2+} and Na^{+} with an average of 48.72%, 37.63%, respectively. In the Group 3 waters, the γNa/γCl varies from 0.06 to 0.91 with an average of 0.42, and the γ(Cl–Na)/γMg varies from 1.56 to 16.60 with an average of 5.33, the 100 × $\gamma SO_4/\gamma Cl$ varies from 0.24 to 8.42 with an average of 3.38 (Fig. 6; Table 1).

4.3. Crude oil geochemistry

The relationship between density and viscosity of crude oils in the buried hills is shown in Fig. 7. According to the common standards of oil fields in China, crude oils in the Shulu Sag can be classified into light oil, medium oil, heavy oil, and super heavy oil (Fig. 7; Table 2). The light oils are characterized by low density (the average of 0.836 g/cm^3), low viscosity (the average of 5.67 mPa s), low sulphur content (the average of 0.18%), high wax content (the average of 16.99%) and low resin and asphaltene content (the average of 12.37%) (Table 2). The light oils were mainly produced from wells JG1 and JG2 on the Paleo-uplift and wells JG6 and JG33 on the Northern Slope. The only medium oil is produced from well JG14-1 on the Northern Slope, and its physical properties are slightly worse than light oil (Fig. 7; Table 2). The heavy oils mainly produced from wells JG21, JG22, JG23 on the Southern Slope are characterized by higher density (the average of 0.966 g/cm^3), higher viscosity (the average of 2231.00 mPa s), higher sulphur content (the average of 1.29%), lower wax content (the average of 7.08%) and higher resin and asphaltene content (the average of 57.93%) (Fig. 7; Table 2). The JG21 oils have better quality than other heavy oils and are similar to medium oil (Fig. 7). The super heavy oils have the highest density (the average of 1.031 g/cm^3), the highest viscosity (the average of 5594.49 mPa s), the highest sulphur content (the average of 1.72%), the lowest wax content (the average of 4.53%) and high resin and asphaltene content (the average of 57.82%) (Fig. 7; Table 2). The super heavy oils were mainly produced from wells J7, J34, and nearby wells on the Southern Slope, which did not form commercial oil.

The oil quality in different regions has obvious differences. The oils from the Paleo-uplift are light, the oils from the Northern Slope are light to medium, and the oils from the Southern Slope are heavy to super-heavy (Fig. 7; Table 2). The GC-MS of typical crude oils from the buried hills is shown in Fig. 8. All crude oils have similar characteristics of sterane and terpane and different distributions of normal alkanes. According to the maturity parameters such as the 20S/(20S + 20R) and ββ/(αα+ββ) for C_{29} steranes, the maturity of crude oils varies slightly, which are mainly low-mature oils with a small number of mature oils from Paleo-uplift (Table 3; Zhou et al., 2021).

5. Discussion

5.1. Origin of formation water

The coupling of chemical and isotope composition and trace elements of the formation water is a common tool to study its origin and evolution (Lüders et al., 2010; Bagheri et al., 2014; Saller and Stueber, 2018; Yu et al., 2019, 2021). However, sampling of the original formation waters in many older oilfields mainly occurs in the early stages of drilling, and only a simple chemical analysis is performed (An et al., 2021). Resampling for further analysis is difficult because formation water has been contaminated during development. Studies on the origin and evolution of formation water based on chemical composition alone in the absence of isotopic data have been reported many times (Grasby et al., 2012; Cortes et al., 2016; Li and Zeng, 2017; Yu et al., 2020; Dong et al., 2020; An et al., 2021), proving that this approach is feasible for the study of formation water in older oilfields.

In sedimentary basins, the origin and geochemistry of original formation waters depend on the sedimentary environment (An et al., 2021) but can also be altered during geological evolution (Panno et al., 2013; Li and Cai, 2017; Saller and Stueber, 2018; Engle et al., 2020; Hermides et al., 2020). There are three main reasons for the changes in salinity and chemical composition of formation waters: 1) subaerial evaporation (McCaffrey et al., 1987; Birkle et al., 2009), a common phenomenon as the temperature and pressure gradually increases along with the burial of formation. With a certain degree of evaporation, the concentration of all ions in the water increases (Rittenhouse, 1967). 2) water-rock interactions occur during the flow or stay of water in the subsurface, resulting in salinity and chemical components changes (Birkle et al., 2009; Yu et al., 2021; An et al., 2021). 3) intrusion of meteoric water with low salinity can dilute the primary formation waters (Birkle and Aguilar Maruri, 2003; Panno et al., 2013; Chen et al., 2018). Moreover, meteoric water can significantly affect water chemistry through leaching minerals due to its strong dissolution ability (Moore and Wade,

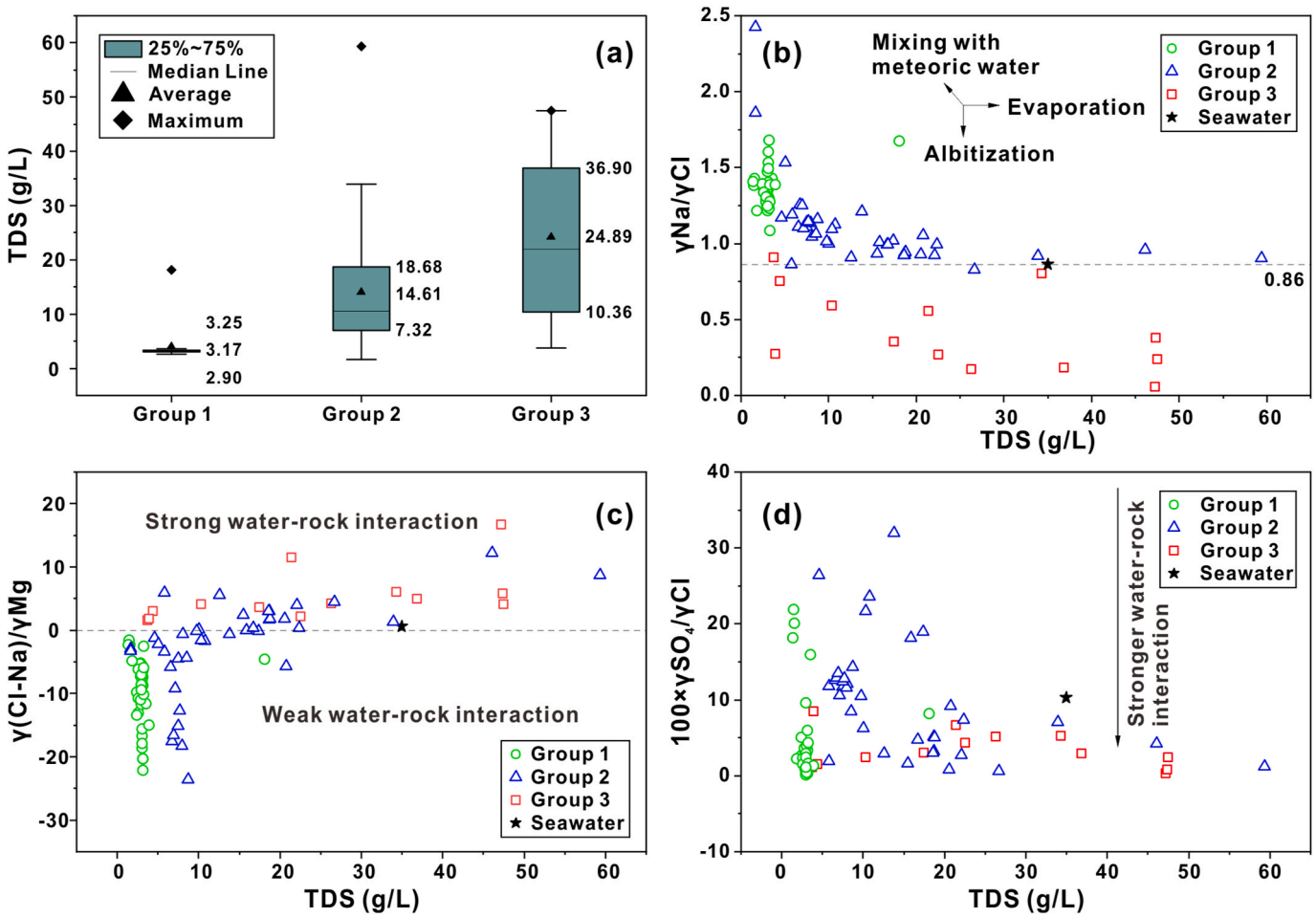

Fig. 6. (a) The box plot for TDS of different formation waters from the buried hills in the Shulu Sag. (b–d) The scatter plot of the characteristic coefficients with the TDS for formation waters. The characteristic coefficients include (b) γNa/γCl, (c) γ(Cl–Na)/γMg, (d) 100 × γSO_4/γCl and are calculated by the ion concentration that is in meq/L.

Table 1
The geochemistry of three types of formation waters in the buried hills of Shulu Sag. The numbers in parentheses are averages.

Water type	TDS (g/L)	Hydrochemical type		Main ions (% of meq)	Characteristic coefficients			Location
		Shukraft classification	Sulin classification		γNa/γCl	γ(Cl–Na)/γMg	100 × γSO_4/γCl	
Group 1	3.17	Na–HCO_3·Cl	$NaHCO_3$	Cl^-: 66.95% HCO_3^-: 30.73% Na^+: 89.69%	1.09–1.68 (1.35)	−22.20 ~ −1.61 (−9.82)	0.12–21.83 (3.79)	Ningjin Uplift, Western Slope
Group 2	14.61	Na–Cl	$CaCl_2$; $NaSO_4$; $NaHCO_3$	Cl^-: 81.87% Na^+: 86.23%	0.83–2.42 (1.10)	−23.67–12.15 (−2.38)	0.55–31.94 (9.92)	Paleo-uplift, Southern Slope
Group 3	24.89	Ca·Na–Cl	$CaCl_2$	Cl^-: 90.99% Na^+: 37.63% Ca^{2+}: 48.72%	0.06–0.91 (0.42)	1.56–16.60 (5.33)	0.24–8.42 (3.38)	Paleo-uplift, Northern Slope

2013).

Although the primary formation waters in the buried hills originate from ancient seawater, the TDS of the formation waters is significantly lower than that of modern seawater (Fig. 3), which suggests that the primary formation waters have been diluted and substituted by meteoric water (Saller and Stueber, 2018). Since the Late Paleozoic, the buried hill strata have been uplifted, weathered, and denuded for hundreds of millions of years, providing favorable conditions for the intrusion of meteoric water. However, the geochemical heterogeneity of current formation waters indicates that they have undergone different evolution processes after being diluted (Fig. 4; Fig. 6; Yu et al., 2021).

5.1.1. Characteristic coefficients

The characteristic coefficients, including γNa/γCl, γ(Cl–Na)/γMg and 100 × γSO_4/γCl, are used to evaluate the hydrodynamic environment and the degree of water-rock interactions (Li and Zeng, 2017; Yu et al., 2019, 2020). Generally, halite precipitation caused by evaporation beyond halite saturation level may cause the γNa/γCl ratio below 0.86 (Bagheri et al., 2014). On the contrary, halite dissolution may result in the γNa/γCl ratio approaching 1 (Yu et al., 2021). In addition, intense water-rock interactions also cause the lower γNa/γCl, while the intrusion of meteoric water makes the γNa/γCl ratio greater than 1 (Li and Jiang, 2013; Li and Zeng, 2017; An et al., 2021). The γ(Cl–Na)/γMg is greater than 0, indicating that the formation waters have experienced

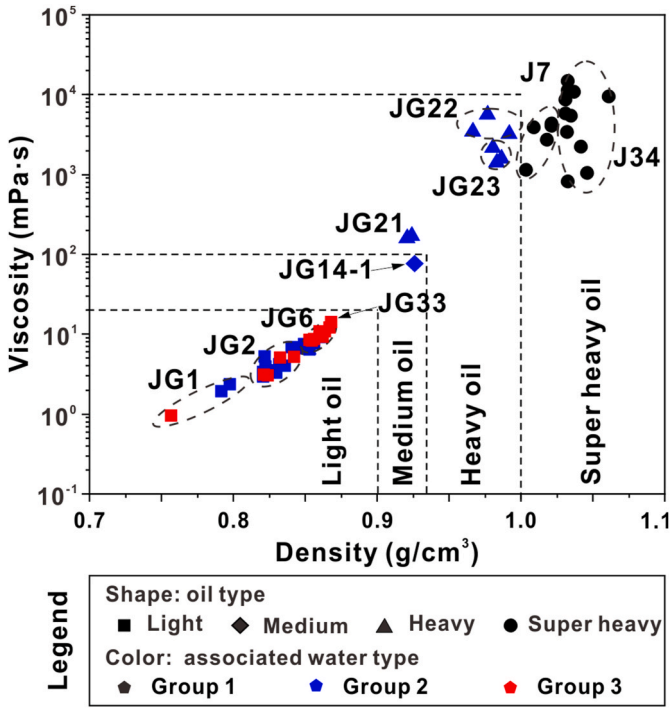

Fig. 7. The scatter plot of density and viscosity of crude oils from DST analysis in the buried hills of the Shulu Sag. Four types of crude oils represented by different shapes are identified based on density and viscosity. The different colors represent the type of formation waters associated with the oils in the test interval. (For interpretation of the references to color in this figure legend, the reader is referred to the Web version of this article.)

strong water-rock interactions. The higher the value is, the better the formation sealing is (Li and Jiang, 2013; Li and Zeng, 2017). The γ(Cl–Na)/γMg is less than 0, indicating the intrusion of meteoric water and weak water-rock interactions. The 100 × $\gamma SO_4/\gamma Cl$ represents the degree of desulfurization of formation waters. The closer the value is to 0, the more intense the water-rock interactions are (Yu et al., 2019; An et al., 2021).

As shown in Fig. 6 and Table 1, the γNa/γCl of Group 1 waters is greater than 1, the γ(Cl–Na)/γMg is lower than 0, and the 100 × $\gamma SO_4/\gamma Cl$ is dispersed with an average of 3.79, indicating that Group 1 waters are in an open hydrodynamic environment and are affected by meteoric water (Li and Zeng, 2017; Xu et al., 2019). The γNa/γCl of Group 3 waters is lower than 0.86, the γ(Cl–Na)/γMg is greater than 0, and the 100 × $\gamma SO_4/\gamma Cl$ is concentrated with an average of 3.38. The maximum concentration of Cl^- for the formation waters in the study area is 35.2 g/L, which is far below the halite saturation level (178 g/L; Panno et al., 2013). Therefore, the lower γNa/γCl is caused by intense water-rock interactions rather than extreme evaporation beyond the halite saturation level (Li and Zeng, 2017). Moreover, the γ(Cl–Na)/γMg and 100 × $\gamma SO_4/\gamma Cl$ also indicate that the formation of Group 3 waters is mainly related to the intense water-rock interactions under the closed environment (Li and Zeng, 2017; Yu et al., 2020). According to the γNa/γCl, some of Group 2 waters follow the evaporation trend, and the other portion of Group 2 waters has the feature of meteoric water (Fig. 6b). The TDS and characteristic coefficients of the Group 2 waters mainly fall in between Group 1 waters and Group 3 waters (Fig. 4; Fig. 6; Table 1), indicating that the Group 2 waters are formed by the mixture of Group 1 waters and Group 3 waters under a semi-open environment (Connolly et al., 1990; Li and Zeng, 2017; Dong et al., 2020).

5.1.2. Water-rock interactions

The cations such as Na^+, K^+, Mg^{2+}, and Ca^{2+} usually occur in the formation water as ion pairs with Cl^- (Drever, 1988). Therefore, the relationship between Cl^- and other cations is appropriate to reveal the hydrogeochemical processes in the formation waters (Lüders et al., 2010; Sanjuan et al., 2016; Saller and Stueber, 2018; Papazotos et al., 2019). In addition, the relationship between Ca_{excess} and $Na_{deficit}$, which Davisson and Criss (1996) proposed based on the study of more than 800 formation waters from multiple basins, is also used to reveal the water-rock interactions (Birkle et al., 2009; Li and Cai, 2017; Chen et al., 2018; Yu et al., 2021). Similarly, the relationship between Ca_{excess} and $Mg_{deficit}$ is used to identify the processes of dolomitization (Birkle et al., 2009; Saller and Stueber, 2018; Yu et al., 2019). The calculation method of Ca_{excess}, $Na_{deficit}$, and $Mg_{deficit}$ refers to Davisson and Criss (1996) and Yu et al. (2019).

As shown in Fig. 9a, Cl^- concentration of formation waters is positively correlated with Na^+. However, not all data points coincide highly with the halite dissolution or seawater evaporation lines (Fig. 9a). Any deviation cannot be explained by seawater evaporation or halite dissolution alone (Grasby et al., 2012). Compared with formation waters in other basins, such as Tarim Basin in China, Sverdrup Basin in Canada, and Permian Basin in the United States (Grasby et al., 2012; Li and Cai, 2017; Saller and Stueber, 2018; Chen et al., 2018), the TDS of formation waters in the study area is lower by more than an order of magnitude, which suggests that evaporation and halite dissolution may not be as significant as in the other area. The distribution of Mg^{2+} and Ca^{2+} away from the seawater evaporation line indicate the influence of other water-rock interactions, which are discussed below (Fig. 9b–c).

Group 1 waters are mainly distributed above the halite dissolution line with Cl^- deficit and Na^+ excess (Fig. 9a). In addition, compared with seawater evaporation, the Group 1 waters have Na^+ enrichment and Mg^{2+} depletion characteristics (Fig. 9). In the diagram of Ca_{excess}-$Na_{deficit}$, Group 1 waters are characterized by Na^+ excess and slight Ca^{2+} excess (Fig. 10a–b). The origin of Cl^- and Na^+ is usually related to halite dissolution and the subaerial evaporation of seawater (Li and Cai, 2017). In addition, the dissolution of sodium-rich silicate minerals by meteoric water will also lead to the Na^+ enrichment and release the equal moles of HCO_3^- into the formation water (Du et al., 2010). The ion exchange between rock and water will also make Na^+ relatively enriched (Bolaji et al., 2021). The good linear relationship between HCO_3^- and excess

Table 2
The physical properties of crude oils in the buried hills of Shulu Sag. The numbers in parentheses are averages. n.d. = no data.

Oil type	Sample number	Density (g/cm³)	Viscosity (mPa·s)	Resin + Asphaltenes (%)	Sulphur content (%)	Wax content (%)	Solidification point (°C)	Associated water type	Location
Light oil	34	0.757–0.868 (0.836)	0.95–13.94 (5.67)	2.70–29.33 (12.37)	0.04–0.45 (0.18)	9.50–44.80 (16.99)	5.0–38.0 (26.2)	Group 3 Group 2	Paleo-uplift Northern Slope
Medium oil	1	0.927	75.6	37.00	0.42	7.50	n.d.	Group 2	Northern Slope
Heavy oil	8	0.921–0.992 (0.966)	158.81–5617.00 (2231.00)	35.16–78.25 (57.93)	0.86–1.64 (1.29)	4.80–14.04 (7.08)	2.0–5.0 (3.5)	Group 2	Southern Slope
Super heavy oil	16	1.004–1.062 (1.031)	816.00–14690.00 (5594.49)	47.56–71.20 (57.82)	1.14–2.89 (1.72)	0.35–12.84 (4.53)	24.0–56.0 (40.9)	Group 1	Southern Slope

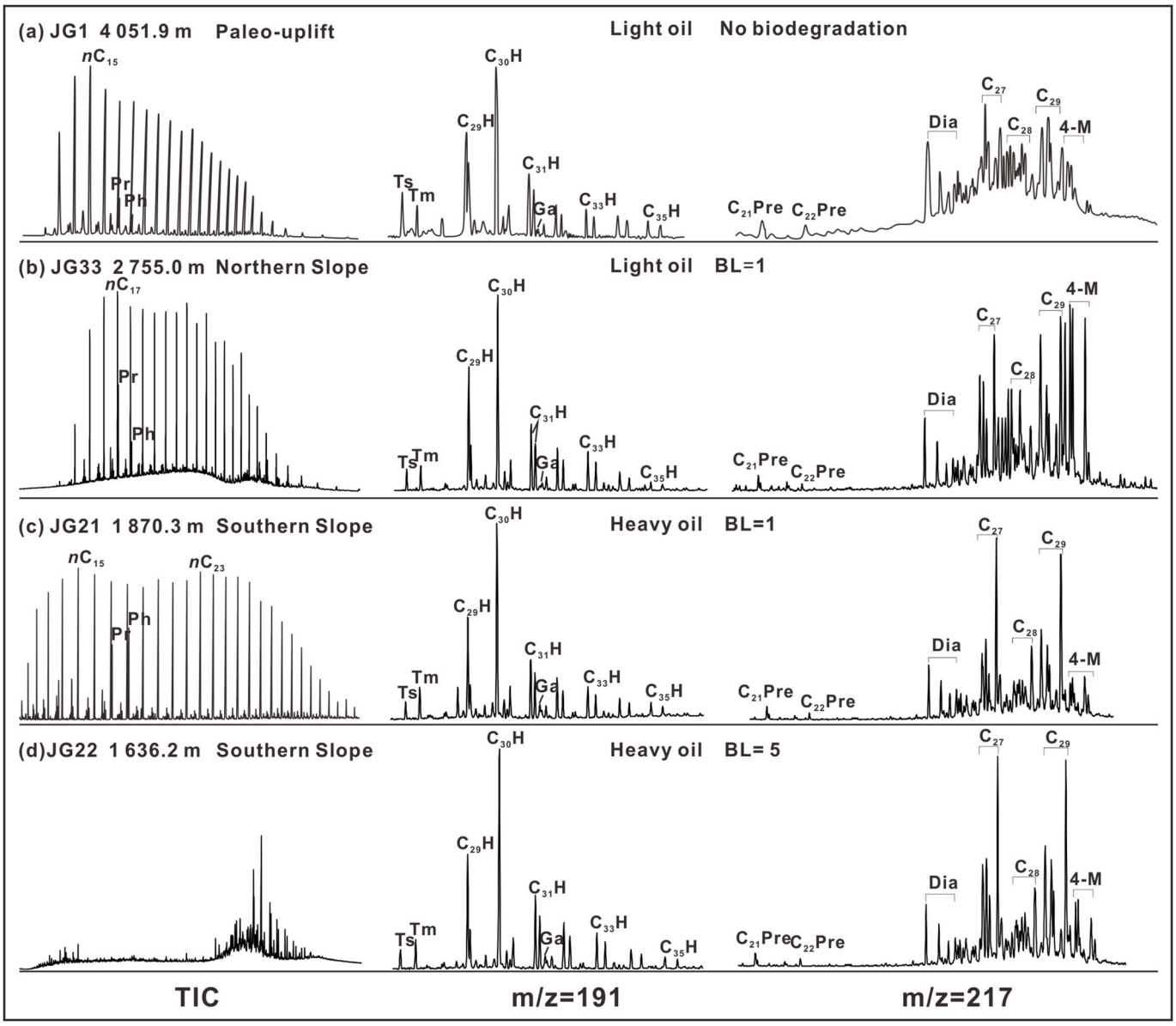

Fig. 8. GC-MS for saturated hydrocarbon of crude oils in the Shulu Sag's buried hills. The similar characteristics of sterane and terpane for crude oils indicate that they have the same source. The different characteristics of normal alkanes show that biodegradation level ranges from non-biodegraded to moderately-biodegraded. BL represents biodegradation level. Ga represents gammacerane. $C_{30}H$ represents C_{30} hopane, $C_{31}H$–$C_{35}H$ represents C_{31}–C_{35} homohopane isomers. C_{27}–C_{29} represents C_{27}–C_{29} sterane. 4-M represents 4-Methylsteranes. Dia represents diasteranes. C_{21} Pre and C_{22} Pre represent C_{21} pregnanes and C_{22} pregnanes, respectively.

Table 3
The maturity parameters and biodegradation level of crude oils in the buried hills of Shulu Sag.

Oil sample	Well location	Depth (m)	Maturity parameters		Biodegradation level	Associated water type
			20S/(20S + 20R)-C_{29}St	ββ/(αα+ββ)-C_{29}St		
JG1	Paleo-uplift	4051.9	0.54	0.45	0	Group 2
JG33	Northern slope	2755.0	0.47	0.33	1	Group 3
JG21	Southern slope	1870.3	0.34	0.31	1	Group 2
JG22	Southern slope	1636.2	0.36	0.35	5	Group 2

Na^+ ($Na^+{}_{excess}/HCO_3^-$ molar ratio is approximately 1) in the Group 1 waters (Fig. 11a) suggests that the dissolution of sodium-rich silicate by meteoric water may be the primary geochemical process to form the Group 1 waters, and the excess Na^+ combines with HCO_3^- to form the $NaHCO_3$ water, which is the main type in the Group 1 waters (Table 1). The Mg^{2+} depletion in the Group 1 water may be attributed to the dilution of meteoric water.

Group 3 waters are located below the halite dissolution and seawater evaporation line with Cl^- excess and Na^+ deficit (Fig. 9a). Moreover, Group 3 waters have Ca^{2+} enrichment and Na^+ depletion characteristics compared with seawater evaporation (Fig. 9). There is a positive linear relationship between excess Cl^- and Ca^{2+} in the Group 3 waters (Fig. 11b). The $Ca^{2+}/Cl^-{}_{excess}$ molar ratio is approximately 0.5, indicating that excess Cl^- combines with Ca^{2+} to form the essential $CaCl_2$

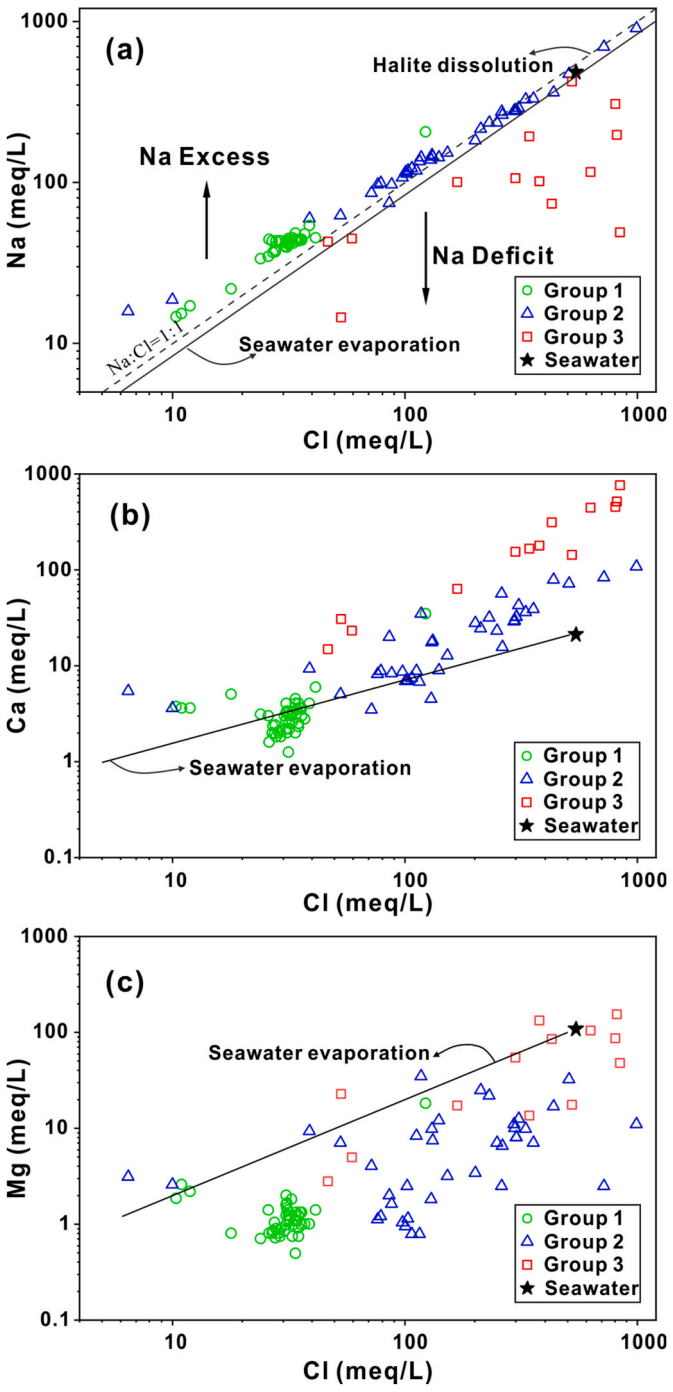

Fig. 9. The scatter plots of Cl^- vs. main cations (Na^+, Ca^{2+}, and Mg^{2+}) of modern seawater and formation waters from the buried hills of the Shulu Sag. The seawater evaporation line and halite dissolution line are from McCaffrey et al. (1987).

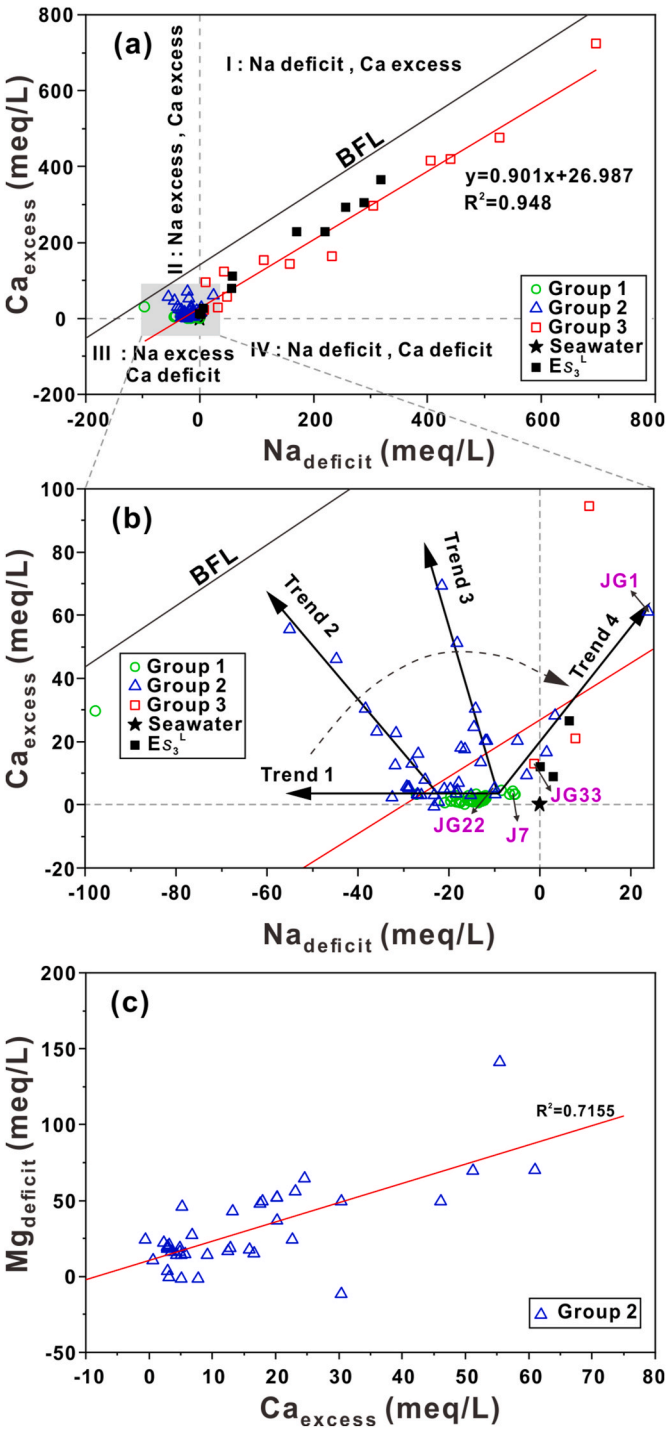

Fig. 10. The plots of (a–b) Ca_{excess} vs. $Na_{deficit}$ and (c) $Mg_{deficit}$ vs. Ca_{excess} of formation waters from the buried hills of the Shulu Sag. (b) is an enlarged view of the shaded part in (a). The Basinal Fluid Line (BFL) is from Davisson and Criss (1996).

water in the Group 3 waters (Table 1). Furthermore, Fig. 10a shows an apparent Ca_{excess}-$Na_{deficit}$ linear relationship ($R^2 = 0.948$) in the Group 3 waters. The slope is approximately 1, which is the same as the Basinal Fluid Line (BFL, $Ca_{excess} = 0.967\ Na_{deficit} + 140.3$, $R^2 = 0.981$) proposed by Davisson and Criss (1996), meaning a net cation exchange ratio of two Na^+ for one Ca^{2+}. It is believed that only albitization of plagioclase is the reasonable explanation for this feature (Boles, 1982; Davisson and Criss, 1996). Although the plagioclase in buried hill strata is rare, the albitization of plagioclase is likely to be the primary geochemical process for forming Group 3 waters (Li and Cai, 2017; Chen et al., 2018) because the Ca_{excess}-$Na_{deficit}$ linear relationship is independent of basin lithology (Davisson and Criss, 1996). Such fluids with Ca_{excess}-$Na_{deficit}$ linear relationship are often found in the feldspar-poor rocks, such as carbonate rocks, which can be explained by fluid circulation through the feldspar-sufficient zones (Davisson and Criss, 1996). For example, some scholars believe that the Ordovician waters with similar characteristics in the carbonate reservoirs of Tarim Basin migrate from the deep Cambrian mudstone (Li and Cai, 2017; Chen et al., 2018). Therefore, the formation of Group 3 waters in the buried hills may be attributed to fluid

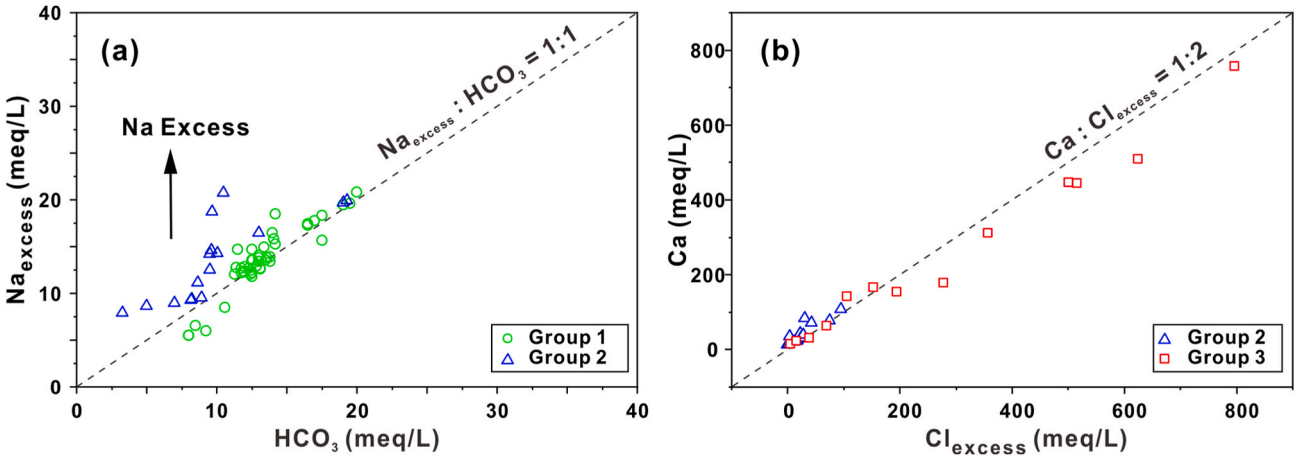

Fig. 11. The plots of (a) HCO_3^- vs. Na_{excess} and (b) Cl_{excess} vs. Ca^{2+} of formation waters from the buried hills of the Shulu Sag. The Na_{excess} is calculated by subtracting the content of Cl^- from the content of Na^+. The Cl_{excess} is calculated by subtracting the content of Na^+ from the content of Cl^-.

migration from the lower part of Mbr 3 of the Shahejie Fm, which has waters with Na^+ deficit and Ca^{2+} excess (Fig. 10a). In addition, the high salinity of Group 3 waters may have resulted from further evaporation and concentration in a closed environment.

Some Group 2 waters are distributed on the halite dissolution line, which shows that halite dissolution contributes to forming the Group 2 waters, but other samples have deviated. Some Group 2 waters are distributed above the halite dissolution line with Cl^- deficit and Na^+ excess (Fig. 9a), similar to Group 1 waters. The difference is that these Group 2 waters still have excess Na^+ relative to HCO_3^-, which can be attributed to Na^+ enrichment or HCO_3^- depletion (Fig. 11a). The enrichment of Na^+ may be related to ion exchange, while the depletion of HCO_3^- may be related to calcite precipitation (Cheng et al., 2006). In addition to combining with HCO_3^- to form $NaHCO_3$ water, excess Na^+ can also combine with SO_4^{2-} to form Na_2SO_4 water in the Group 2 waters (Table 1). The source of SO_4^{2-} may involve the dissolution of gypsum. Another portion of Group 2 waters is located below the halite dissolution line with slight Cl^- excess and slight Na^+ deficit (Fig. 9a). The linear relationship between excess Cl^- and Ca^{2+} indicates that excess Cl^- combines with Ca^{2+} to form the $CaCl_2$ water (Fig. 11b; Table 1), while the low salinity suggests weaker water-rock interactions in Group 2 waters.

Compared with seawater evaporation, the Group 2 waters have Ca^{2+} enrichment and Mg^{2+} depletion characteristics (Fig. 9). The Ca^{2+} enrichment and Mg^{2+} depletion are usually attributed to the dolomitization of calcite (Chen et al., 2018; Yu et al., 2019). As shown in Fig. 9b–c, the increase in Ca^{2+} of the Group 2 waters is the closest to the decrease in Mg^{2+}, suggesting that the dolomitization may also be one of the mechanisms affecting the chemical composition of the Group 2 waters (Birkle et al., 2009; Saller and Stueber, 2018). As shown in Fig. 10c, the good linear relationship ($R^2 = 0.7155$) is observed in the Group 2 waters, and the molar ratio of $Mg_{deficit}$ to Ca_{excess} is about 1.26 (Fig. 10c), indicating that other effects, such as the dilution of meteoric water, cause the Mg^{2+} depletion in the Group 2 waters in addition to dolomitization. Group 2 waters are relatively concentrated with a slight excess of Ca^{2+} and Na^+ in Fig. 10a–b, indicating weaker water-rock interactions. It can be seen from the locally enlarged view that the Group 2 waters have four trends in the diagram of Ca_{excess}-$Na_{deficit}$ (Fig. 10b). Trend 1 is the same as the Group 1 waters and represents Na^+ excess and slight Ca^{2+} excess, which is mainly $NaHCO_3$ water formed by meteoric water. Although Trend 2 and Trend 3 represent Na^+ excess and Ca^{2+} excess, they are Na_2SO_4 water and $CaCl_2$ water, respectively. Trend 4 represents Ca^{2+} excess and Na^+ deficit, which is $CaCl_2$ water with similar characteristics to the Group 3 waters. These characteristics indicate that Trends 2 and 3 are transitional types between Trends 1 and 4, and Group 2 waters are transitional types between Group 1 and Group 3 waters. Therefore, we believe that Group 2 waters are formed by mixing Group 1 and Group 3 waters.

In summary, formation waters from the buried hills in the Shulu Sag have a variety of origins. Group 1 waters came mainly from meteoric water from an open environment based on the lowest TDS, γ(Cl–Na)/γMg, and the highest γNa/γCl. The dilution of meteoric water and the dissolution of sodium-rich silicate are the main hydrogeochemical processes for forming Group 1 waters. Group 3 waters are connate water affected by the formation waters from the Shahejie Fm in a closed environment based on the highest TDS, γ(Cl–Na)/γMg and the lowest γNa/γCl. The albitization of plagioclase is critical for the formation of Group 3 waters in addition to evaporation and concentration in a closed environment. Group 2 waters are formed by mixing meteoric water and connate water in a semi-open environment because the chemical characteristics of Group 2 waters are between Group 1 and Group 3 waters. The water-rock interactions in the Group 2 waters are complex, mainly including dolomitization, halite dissolution, gypsum dissolution, and calcite precipitation.

5.2. Biodegradation level (BL) of crude oil

Biodegradation of crude oil leads to reduced saturated hydrocarbon, wax content, and increased density, viscosity, and sulphur content, negatively affecting oil production and reducing oil value (Head et al., 2003). The physical properties and GC-MS analysis of crude oil in the study area have shown that biodegradation occurs in the reservoirs and significantly affects the oil quality or destroys the oil reservoir (Table 2; Fig. 7; Fig. 8; Fig. 12). Similar sterane and terpane distribution reveal that all crude oils have the same source (Fig. 8). In addition, the maturity-related biomarker parameters show that the maturity of crude oils varies slightly (Table 3). The differences of normal alkanes show that the BL of crude oils ranges from non-biodegraded to moderately-biodegraded (Fig. 8), which is consistent with their density and viscosity, indicating that biodegradation is the leading cause for heterogeneity in oil quality.

In the JG1 light oil from the Paleo-uplift, the normal alkanes, ranging from C_{13} to C_{35}, show a smooth and unimodal distribution (Fig. 8a). Steranes and terpanes are intact. In addition, the wax content and sulphur content are 17.2% and 0.05%, respectively. These characteristics indicate that the JG1 oil is non-biodegraded (Fig. 8a). In the JG33 light oil from the Northern Slope, normal alkanes are slightly depleted with an unresolved complex mixture (UCM). Moreover, isoprenoids, steranes, and terpanes are barely consumed (Fig. 8b). The wax content and sulphur content are 18.9% and 0.23%, respectively. Based on the

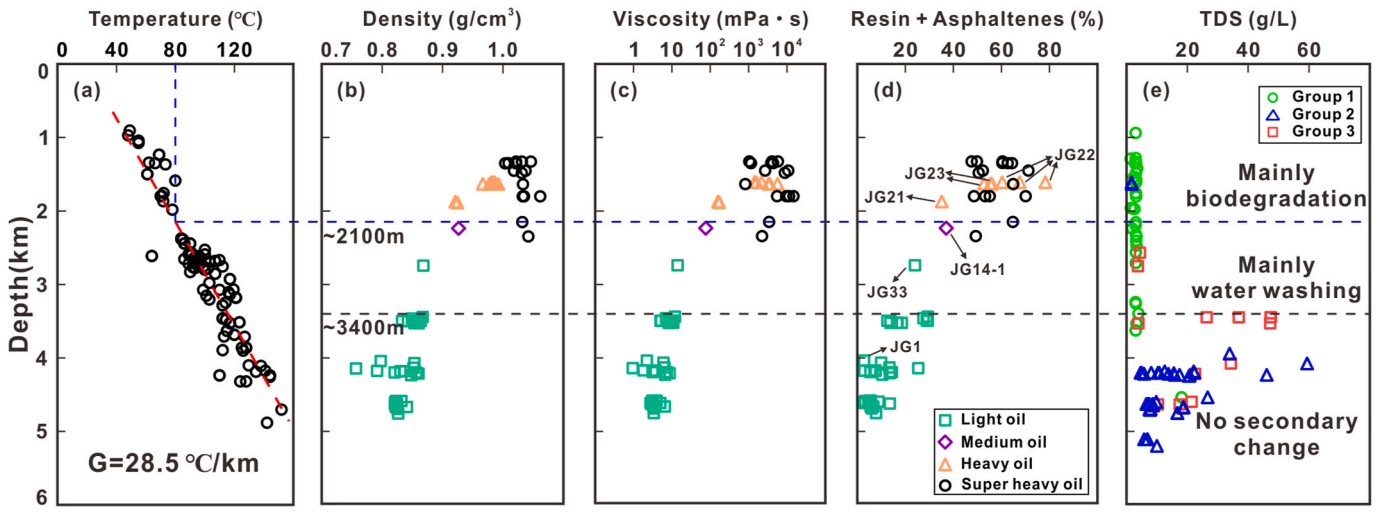

Fig. 12. Reservoir temperature (a), the physical property of crude oil (b–d), and TDS (e) of formation waters vary with depth. (a) The average temperature gradient in the Shulu Sag is about 28.5 °C/km, based on the temperature data collected from PetroChina Huabei Oilfield. (b–c) The density, viscosity, resin, and asphaltenes content decrease as the depth increases, indicating that the secondary changes are related to the depth. Biodegradation and water washing depth are determined based on the average temperature gradient, oil quality, and water chemistry.

evaluation standard of BL outlined by Peters and Moldowan (1993), the JG33 oil is assigned to BL 1. The normal alkanes of JG21 heavy oil from the Southern Slope are characterized by a slight depletion of nC_{16-22} and a pronounced hump (Fig. 8c). Other biomarkers had no noticeable depletion. Moreover, JG21 oil has high wax content (14.04%) and low sulphur content (0.96%). Therefore, the BL of the JG21 oil is 1. The JG22 oil from the Southern Slope is heavy oil with low wax content (5.3%) and high sulphur content (1.64%). The normal alkanes and isoprenoids have been completely consumed, but the steranes and terpanes remain intact (Fig. 8d), which indicates that the BL of JG22 oil is 5 (Peters and Moldowan, 1993). This study lacks GC-MS analysis data for super heavy oil from wells J7 and J34. Based on lower wax content (4.53% on average) and higher sulphur content (1.72% on average) (Table 2), we speculate that super heavy oils have a higher BL than JG22 oil (BL 5).

Water washing is another process to reduce oil quality, which happens simultaneously with biodegradation sometimes (Alkhafaji, 2021). Since the alterations caused by water washing would be overridden by those caused by biodegradation, we cannot easily identify the alterations caused by water washing (Wang et al., 2016). However, it does not mean that the degradation of oil quality in the study area has nothing to do with washing (Wang et al., 2016; Alkhafaji, 2021).

5.3. Secondary changes controlled by water chemistry

It is generally believed that significant biodegradation generally occurs in an aquifer with temperatures below 80 °C under anaerobic conditions (Röling et al., 2003; Larter et al., 2006). In addition, the systematic survey of microorganisms in oil reservoirs suggested that salinity has a greater effect on microbial activity than temperature (Tardy-Jacquenod et al., 1996; Grassia et al., 1996). Previous studies suggest that formation waters originating from meteoric water can provide sufficient nutrients for the survival and metabolism of microorganisms (Rogers et al., 1998; Head et al., 2003). Furthermore, nutrient supply from the aquifer may exert the ultimate control over the degree of degradation (Larter et al., 2006). Therefore, besides the temperature, water chemistry also has essential controls on biodegradation in sedimentary basins (Röling et al., 2003). Water washing is another process related to the formation waters that usually occur under the active hydrodynamic environment (Alkhafaji, 2021), which degrades the oil quality by removing the water-soluble hydrocarbons through contact with water (Peters and Moldowan, 1993; Shelton et al., 2016). According to the origin of formation water, the Group 1 waters in the study area are most conducive to the survival and metabolism of microorganisms, thereby promoting intense secondary changes. In contrast, the Group 3 waters are detrimental to biodegradation because microorganisms may die due to a lack of nutrients. In summary, water chemistry can affect oil quality by controlling biodegradation and water washing, which the following discussion can further confirm.

As shown in Fig. 12b–d, crude oil's density, viscosity, resin and asphaltene content decrease with increasing depth. In the strata above 2100 m, crude oils are heavy and super-heavy oils with high density, viscosity, resin and asphaltenes content. The BL of JG22 and JG21 heavy oil is 5 and 1, respectively. Super heavy oils have a higher BL. On the one hand, the reservoir temperature is lower than 80 °C (Fig. 12a), which benefits microbial activities (Röling et al., 2003; Larter et al., 2006). On the other hand, the corresponding formation waters are mainly Group 1 waters and a small amount of Group 2 waters (the TDS lower than 5.00 g/L) (Fig. 12e), symbolizing adequate nutrients and the active hydrodynamic forces. Therefore, the intense biodegradation accompanying water washing, caused by the strong intrusion of meteoric water, is the main reason for forming heavy and super-heavy oil in the strata above 2100 m.

In the strata from 2100 m to 3400 m depth, the oils are medium oil (JG14-1) and light oil (JG33), with little biodegradation (BL = 1) (Fig. 12b–d). Based on the average temperature gradient (G = 28.5 °C/km), the reservoir temperature in the strata below 2100 m is greater than 80 °C (Fig. 12a), resulting in the death of a large number of microorganisms and limited biodegradation. The corresponding formation waters are mainly Group 1 waters and a small amount of Group 3 waters (Fig. 12e). Based on the previous conclusion (Xiang et al., 2007), formation water with the TDS below 5.00 g/L in the study area is still favorable for water washing, suggesting that 3400 m is the maximum depth where water washing occurs (Fig. 12e). Therefore, water washing is the main secondary change of crude oil in the strata from 2100 m to 3400 m. The slight depletion of normal alkanes in JG33 oil is attributed to water washing rather than biodegradation.

The oils in the strata below 3400 m are non-biodegraded light oil with low density, viscosity, resin and asphaltenes content, such as JG1 oil (Fig. 12b–d). The corresponding formation waters are mainly Group 3 and Group 2 waters with high salinity (Fig. 12e). High reservoir temperature and high salinity indicate no significant biodegradation and water washing occur in the strata below 3400 m, resulting in the best oil quality. In conclusion, the secondary changes are the main mechanisms by which water affects oil quality.

5.4. The reason for the different oil quality in different regions

Secondary changes can also explain the differences in the oil quality in different regions. The buried hills in the Northern Slope have a considerable burial depth (>2700 m), such as wells JG33 and JG6. The secondary changes are dominated by water washing, resulting in the formation of the light-medium oil reservoirs. On the contrary, the burial depth of the buried hills in the Southern Slope is relatively shallow (<2000 m). The oils not only suffer from water washing but also undergo intense biodegradation, which leads to the formation of heavy and super heavy oils. The buried depth of the Paleo-uplift is more than 4000 m, so the oils are not affected by secondary changes, thus forming light oil reservoirs.

JG22 and JG23 buried hills with commercial oil reservoirs have a similar buried depth to the buried hills around wells J7 and J34 (Fig. 12), but their oils still differ in physical properties (Fig. 13). On the one hand, although the viscosity of crude oil is similar, the latter is denser (Fig. 7; Fig. 13a). On the other hand, compared with the light oils, the solidification point of the latter is increased, while that of the former is decreased (Fig. 13a; Table 2). In general, the solidification point of crude oil is positively correlated with wax content. According to this rule, the solidification point of super-heavy oils should be lowered due to the lowest wax content and highest sulphur content (Fig. 13b). However, the solidification point of super-heavy oils is abnormally high (Fig. 13a; Table 2), which contradicts general understanding. Previous studies suggest that the high solidification point can be attributed to intense water washing rather than biodegradation (Lafargue and Barker, 1988; Kuo, 1994).

Most traps on the western slope are structural traps related to a fault (Fig. 1c). Fault displacement of the reverse fault in wells JG22 and JG23 traps is relatively larger (about 450 m) to weaken the influence of meteoric water on the oil reservoir, thus leading to weaker water washing and the formation of Group 2 waters. Therefore, secondary changes of crude oils in well JG22 and JG23 are mainly biodegradation, causing the solidification point of these oils to decrease as the wax content decrease (Fig. 13). On the contrary, the fault displacement of the reverse faults in wells J34 and J7 traps is small (about 100 m), so the crude oils are still subjected to strong water washing to form super-heavy oils with a high solidification point. This difference indicates that biodegradation accompanied by intense water washing may be the main reason for destroying the oil reservoir in the Shulu Sag. Therefore, it is difficult to form commercial oil reservoirs in the strata above 2100 m unless the intrusion and flow of meteoric water are weakened by other factors such as fault.

5.5. Relationship between water chemistry and oil quality

Based on the above discussion, biodegradation and washing are closely related to water chemistry and lead to four types of crude oils in the Shulu Sag. As expected, there is a clear relationship between oil quality and associated water type in the study area (Fig. 7; Table 2). Group 3 waters are associated with light oils in the study area, and Group 1 waters are associated with super heavy oils (Fig. 7; Table 2). Furthermore, oils associated with Group 2 waters range from light to medium to heavy (Fig. 7; Table 2) because the Group 2 waters are intermediate between Group 1 and Group 3 waters. Specifically, the water associated with JG33 light oil is Group 3 waters with Ca^{2+} excess and slight Na^{+} excess, while the water associated with JG1 light oil is Group 2 waters in Trend 4 (Fig. 10b). The water associated with JG22 heavy oil is Group 2 waters in Trend 3, while the water associated with J7 super heavy oils is Group 1 waters (Fig. 10b). In a word, the more meteoric the associated water, the more degraded the oil (Bockmeulen et al., 1983). It suggests that oil quality can be evaluated by water type because the formation water is sensitive to the change in the hydrodynamic environment.

In addition, the oil reservoir distribution is also closely related to water type. The oil reservoirs in the buried hills are mainly distributed in the areas with Group 2 waters and Group 3 waters, such as wells JG1, JG2, JG6, JG22. No commercial oil reservoirs are discovered in the buried hills with Group 1 waters, such as wells J7 and J34. The possible reasons are 1) strong hydrodynamic effects related to Group 1 waters restricted the oil migration from sag to the western buried hills; 2) oil reservoirs had been destroyed by biodegradation and water washing in an open hydrodynamic environment. Other members of the research group revealed the presence of the paleo-oil-water contact (1990 m) and the present oil-water contact (1790 m) of the oil reservoir in well JG22 in the Southern Slope through the Quantitative Fluorescence Technology (QFT) (unpublished data). For detailed principles about QFT, please refer to Liu et al. (2017). Since no strong tectonic movement occurs in the study area during the hydrocarbon charging (5–0 Ma), the adjustment of the oil-water contact and poor oil quality in the JG22 oil reservoir can be attributed to the destruction of the oil reservoir by formation waters.

In summary, the hydrodynamic environment is the main factor for controlling hydrocarbon preservation and accumulation in the study area. Water chemistry can make a good response to the hydrodynamic environment change, thus being used as a reference for oil and gas exploration. Buried hills with Group 3 waters should be the highest priority for further exploration, whose oil reservoirs are dominated by light oil with high commercial value. Although the oil quality is poor, the slope's buried hills with Group 2 waters can be secondary targets. It

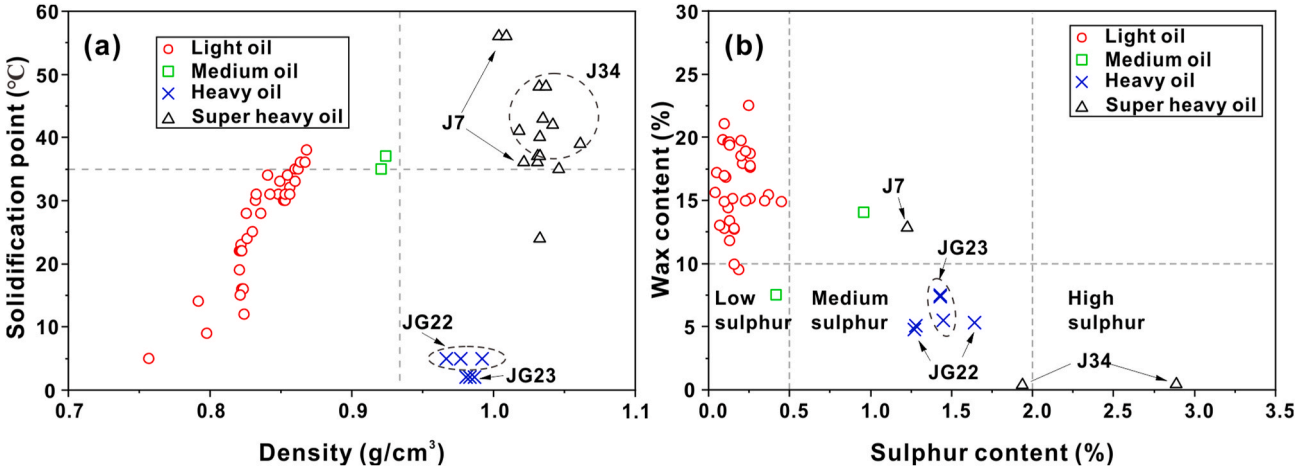

Fig. 13. Scatter plots of (a) Density vs. Solidification point and (b) Sulphur content vs. Wax content of crude oils from the buried hill of the Shulu Sag.

is recommended to avoid arranging wells in the buried hills with Group 1 waters.

5.6. Evolution mode of formation water and its relationship to hydrocarbon accumulation

The formation and evolution of water run through the whole process of hydrocarbon migration, accumulation, and preservation (Li and Cai, 2017; Chen et al., 2018). Based on the above discussion, the hydrogeological model about the origin, evolution, and flow of formation waters is proposed to explain the relationship between water evolution and hydrocarbon accumulation (Fig. 14).

The Ordovician-Cambrian strata were deposited in the marine environment (Xiang et al., 2021), the Permo-Carboniferous strata were deposited in the marine-continental transitional environment. Therefore, the primary formation waters were likely to be ancient seawater entrapped during deposition (Fig. 14a). Before the deposition of Cenozoic strata, buried hill strata were uplifted and denuded for a long time under the action of regional tectonic movements such as Caledonian, Indosinian, and Yanshan (Fig. 14a). The primary formation waters were seriously diluted or substituted by meteoric water during the long-term denudation (Fig. 14a–b), as reflected by the much lower TDS than modern seawater.

In the Paleogene, the Paleo-uplift was deeply buried due to the

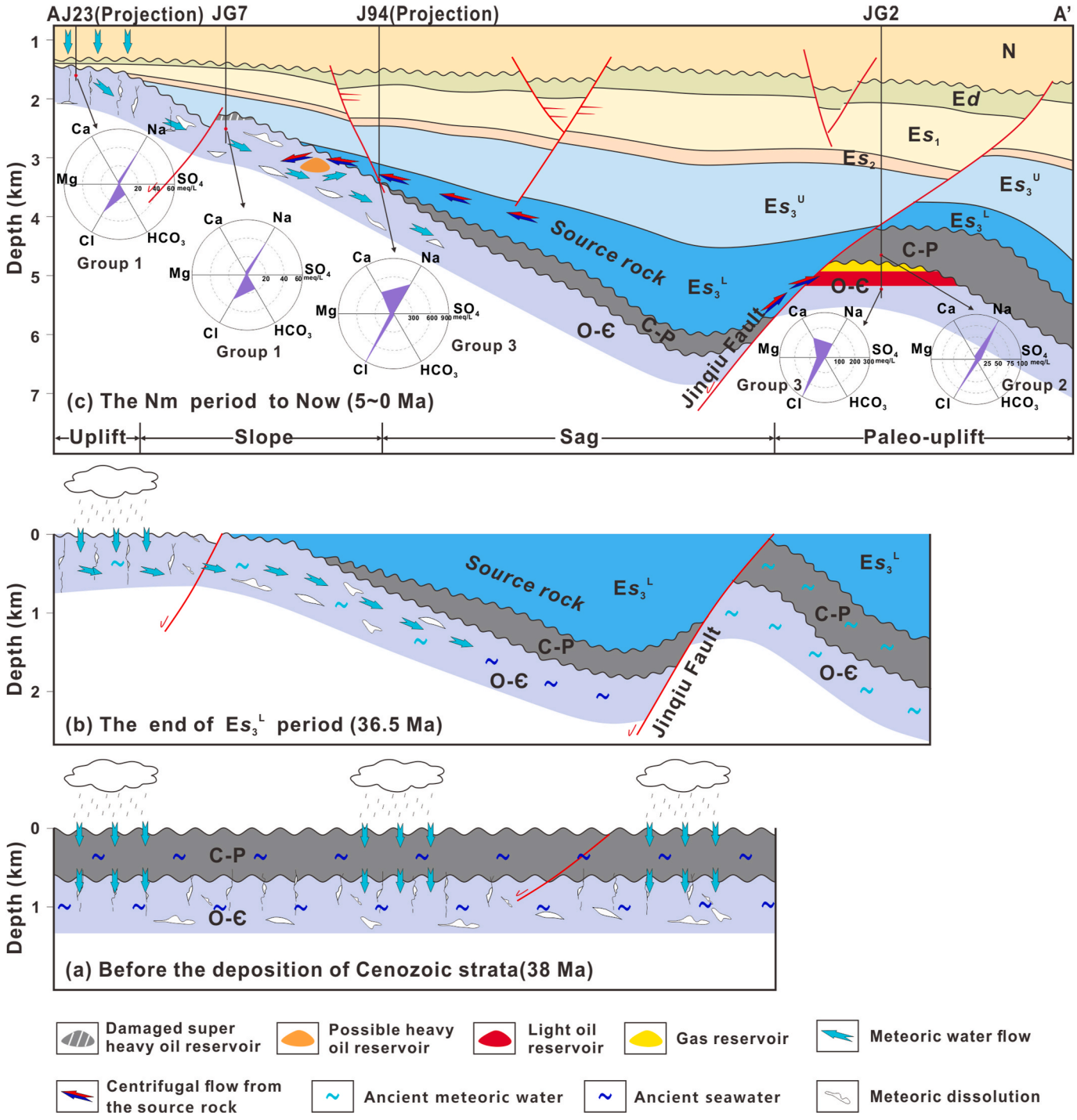

Fig. 14. Evolution of fluid flow of formation waters from the buried hills in the Shulu Sag (AA′ location is shown in Fig.1b).

intense activity of the Xinhe boundary fault, accompanied by rapid deposition in the lower part of Mbr 3 of the Shahejie Fm (Fig. 14b; Jiang et al., 2007). With the increase of temperature and pressure, the formation water of the Paleo-uplift began to evaporate in the closed hydrodynamic environment and react with the surrounding rocks, leading to the increase of salinity. In contrast, the Ningjin Uplift and Western Slope were uplifted and directly connected with the surface water system (Fig. 14b). The meteoric water enters the buried hills from the Ningjin Uplift as a result of gravity flow to form karst reservoirs and the Group 1 waters (Fig. 14b; Xiang et al., 2021).

Since the Neogene Minghuazhen Fm period (5–0 Ma), the source rocks of the Shahejie Fm have entered the “oil window" and generated many hydrocarbons to form centrifugal flow driven by overpressure (Fig. 14c; Xie et al., 2006; Cai et al., 2020; Xiang et al., 2021). Centrifugal flow refers to the fluid that flows from the basin’s center to the edge due to compaction (Li, 2016). During hydrocarbon charging, the hydrocarbons took the formation waters of the Mbr 3 of the Shahejie Fm as the carrier to flow to the Western Slope and the Paleo-uplift (Fig. 14c). Simultaneously, meteoric water driven by gravity hindered the hydrocarbon from flowing to the Western Slope and destroyed the oil reservoirs through biodegradation and water washing to form super heavy oils, such as wells J7 and J34 (Fig. 14c). However, in some buried hills, such as JG21, JG22, and JG23 oil reservoirs, large fault displacement weakens the power of gravity flow, allowing centrifugal flow and meteoric water to mix here to form the Group 2 waters and heavy oil reservoirs (Fig. 14c). The depth of Group 2 waters on the slope depends on the power and velocity of gravity flow and centrifugal flow. Furthermore, the centrifugal flow migrated to the Paleo-uplift to form Group 3 waters (Fig. 14c). The ancient meteoric waters in the Paleo-uplift were affected by the formation waters of the Shahejie Fm to form some Group 2 waters (Fig. 14c). The hydrocarbons are accumulated in the Paleo-uplift and preserved in a closed environment to form light oil reservoirs, such as wells JG1 and JG2.

6. Conclusion

Formation water is the critical factor in controlling the accumulation and preservation of hydrocarbons in the buried hills of the Shulu Sag, which can be used as a reference for hydrocarbon exploration. As a result of the perennial denudation, meteoric water seriously diluted or even replaced the primary formation waters in the buried hills. Three geochemical groups of formation waters with different origins were identified by geochemistry analysis. The Group 1 waters are related to meteoric water, whose chemical compositions are mainly controlled by the dissolution of sodium-rich silicate minerals, representing an open hydrodynamic environment with poor oil and gas preservation. The Group 3 waters are connate water, whose chemical compositions are mainly controlled by the albitization of plagioclase, representing a closed hydrodynamic environment with the best hydrocarbon preservation. Group 2 waters are formed by mixing meteoric and connate water, representing a semi-open hydrodynamic environment with intermediate hydrocarbon preservation.

The clear corresponding relationship between oil quality and associated water type shows that water chemistry significantly affects the oil quality and distribution in the Shulu Sag through secondary changes that occurred in the hydrocarbon migration and accumulation. Biodegradation is the dominant effect in the strata above 2100 m. Water washing is dominant in the depth range of 2100–3400 m, and there are no noticeable secondary changes in the strata below 3400 m. Biodegradation and water washing controlled by the water chemistry are the main reasons for the different oil quality in different blocks, which is also an essential factor that affects whether oil and gas can effectively accumulate.

The evolution of formation water can reflect the process of hydrocarbon accumulation. Meteoric waters flowed into the buried hills from Ningjin Uplift as a result of gravity flow, resulting in intense secondary changes, destruction of the oil reservoirs, and the formation of Group 1 waters. The centrifugal flow driven by overpressure flows in two directions from the source rocks, one is to the western slope and mixes with Group 1 waters to form Group 2 waters and heavy oil reservoirs, and the other is to the paleo-uplift to form Group 2 and Group 3 waters and light oil reservoirs. Water chemistry is sensitive to the hydrodynamic environment change and can be used as a reference for oil and gas exploration. Buried hills with Group 3 waters should be the highest priority for further exploration, whose oil reservoirs are dominated by light oil with high commercial value. Although the oil quality is poor, buried hills with Group 2 waters in the slope can be secondary targets. In comparison, the buried hills with Group 1 waters representing the open environment should be avoided for oil and gas exploration.

In this study, the relationship between water chemistry and hydrocarbon preservation is further confirmed by simultaneously considering the geochemistry of formation water and crude oil. Our result and method can help understand water-rock interactions, predict oil quality and distribution, and further aids hydrocarbon exploration. Moreover, the chemical composition analysis of formation water is very economical to be widely used in evaluating oil and gas preservation.

Credit author statement

Chuan Cai: Data curation, Formal analysis, Investigation, Writing-Original Draft. Nansheng Qiu: Funding acquisition, Investigation, Writing-Reviewing and Editing. Nian Liu: Writing- Reviewing and Editing, Validation. Zhenming Li: Validation, Editing. Yuanjie Wang: Project administration, Reviewing, Resources, Zhanwen Yu: Project administration, Reviewing, Resources. Ting Gao and Yaxian Jiao: Resources.

Declaration of competing interest

The authors declare that they have no known competing financial interests or personal relationships that could have appeared to influence the work reported in this paper.

Acknowledgements

This work was supported by the PetroChina Key Project (HBYT-YJY-2018-JS-177) and the CNPC Science & Technology Major Project (2017E-15). We appreciate the PetroChina Huabei Oilfield Company and many individuals for their support in sample and data collection. The authors are grateful to anonymous reviewers and editors for their constructive comments on improving the paper.

Appendix A. Supplementary data

Supplementary data to this article can be found online at https://doi.org/10.1016/j.petrol.2021.110057.

References

Al-Hajeri, M.M., Bowden, S.A., 2017. Application of formation water geochemistry to assess seal integrity of the Gotnia Formation, Kuwait. Arabian J. Geosci. 10, 56. https://doi.org/10.1007/s12517-017-2842-2.

Alkhafaji, M.W., 2021. Biomarker assessment of oil biodegradation, water washing, and source rock characteristics of oil seeps from the Foothill Zone along the Tigris River, Northern Iraq. J. Petrol. Sci. Eng. 197, 107946. https://doi.org/10.1016/j.petrol.2020.107946.

An, T., et al., 2021. Water-rock interactions and origin of formation water in the bohai Bay Basin: a case study of the cenozoic formation in bonan sag. Interpretation 9 (2), T475–T493. https://doi.org/10.1190/INT-2020-0181.1.

Bagheri, R., Nadri, A., Raeisi, E., Eggenkamp, H.G.M., Kazemi, G.A., Montaseri, A., 2014. Hydrochemical and isotopic ($\delta^{18}O$, $\delta^{2}H$, $^{87}Sr/^{86}Sr$, $\delta^{37}Cl$ and $\delta^{81}Br$) evidence for the origin of saline formation water in a gas reservoir. Chem. Geol. 384, 62–75. https://doi.org/10.1016/j.chemgeo.2014.06.017.

Belkhiri, L., Boudoukha, A., Mouni, L., Baouz, T., 2011. Statistical categorization geochemical modeling of groundwater in Ain Azel plain (Algeria). J. Afr. Earth Sci. 59 (1), 140–148. https://doi.org/10.1016/j.jafrearsci.2010.09.007.

Birkle, P., Aguilar Maruri, R., 2003. Isotopic indications for the origin of formation water at the Activo Samaria-Sitio Grande oil field, Mexico. J. Geochem. Explor. 78–79 (3), 453–458. https://doi.org/10.1016/S0375-6742(03)00090-6.

Birkle, P., García, B.M., Milland Padrón, C.M., 2009. Origin and evolution of formation water at the Jujo–Tecominoacán oil reservoir, Gulf of Mexico. Part 1: chemical evolution and water-rock interaction. Appl. Geochem. 24 (4), 543–554. https://doi.org/10.1016/j.apgeochem.2008.12.009.

Bockmeulen, H., Barker, C., Dickey, P.A., 1983. Geology and geochemistry of crude oils, Bolivar coastal fields, Venezuela. AAPG (Am. Assoc. Pet. Geol.) Bull. 67 (2), 242–270. https://doi.org/10.1306/03B5ACF5-16D1-11D7-8645000102C1865D.

Bolaji, T.A., Oti, M.N., Onyekonwu, M.O., Bamidele, T., Osuagwu, M., Chiejina, L., Elendu, P., 2021. Preliminary geochemical characterization of saline formation water from Miocene reservoirs, offshore Niger Delta. Heliyon 7, e06281. https://doi.org/10.1016/j.heliyon.2021.e06281.

Boles, J.R., 1982. Active albitization of plagioclase, gulf coast tertiary. Am. J. Sci. 282, 165–180. https://doi.org/10.2475/ajs.282.2.165.

Bozau, E., Sattler, C.D., van Berk, W., 2015. Hydrogeochemical classification of deep formation waters. Appl. Geochem. 52, 23–30. https://doi.org/10.1016/j.apgeochem.2014.10.018.

Cai, C., Qiu, N., Liu, N., Li, Z., Wang, Y., Yu, Z., Jiao, Y., 2020. Unconformity characteristics, hydrocarbon migration, and the accumulation model of the buried hill in the Shulu sag, Jizhong depression. Acta Geol. Sin. 94 (3), 888–904. https://doi.org/10.19762/j.cnki.dizhixuebao.2020102.

Chen, J., et al., 2018. Origin and evolution of oilfield waters in the Tazhong oilfield, Tarim Basin, China, and their relationship to multiple hydrocarbon charging events. Mar. Petrol. Geol. 98, 554–568. https://doi.org/10.1016/j.marpetgeo.2018.09.018.

Cheng, J., McIntosh, J.C., Xie, X., Jiao, J.J., 2006. Hydrochemistry of formation water with implication to diagenetic reactions in Sanzhao depression and Qijia-gulong depression of Songliao Basin, China. J. Geochem. Explor. 88, 86–90. https://doi.org/10.1016/j.gexplo.2005.08.091.

Connolly, C.A., Walter, L.M., Baadsgaard, H., Longstaffe, F.J., 1990. Origin and evolution of formation waters, alberta basin, western Canada sedimentary basin. I. Chemistry. Appl. Geochem. 5 (4), 375–395. https://doi.org/10.1016/0883-2927(90)90016-X.

Cortes, J.E., Muñoz, L.F., Gonzalez, C.A., Niño, J.E., Polo, A., Suspes, A., Siachoque, S.C., Hernández, A., Trujillo, H., 2016. Hydrogeochemistry of the formation waters in the San Francisco field, UMV basin, Colombia – a multivariate statistical approach. J. Hydrol. 539, 113–124. https://doi.org/10.1016/j.jhydrol.2016.05.010.

Davisson, M., Criss, R.E., 1996. Na-Ca-Cl relations in basinal fluids. Geochem. Cosmochim. Acta 60 (15), 2743–2752. https://doi.org/10.1016/0016-7037(96)00143-3.

Dickey, P.A., George, G.O., Barker, C., 1987. Relationships among oils and water compositions in Niger delta. AAPG (Am. Assoc. Pet. Geol.) Bull. 71 (10), 1319–1328. https://doi.org/10.1306/703C806A-1707-11D7-8645000102C1865D.

Dong, Y., et al., 2020. The temperature evaluation of the buried hill geothermal reservoirs in the Jizhong depression, bohai Bay Basin, China. Geofluids 2020, 1–14. https://doi.org/10.1155/2020/4814515.

Drever, J.I., 1988. The Geochemistry of Natural Waters. Prentice Hall, Upper Saddle River, N.J, p. 437.

Du, X., Xie, X., Lu, Y., Zhang, L., Zhang, C., 2010. Hydrogeochemistry of formation water in relation to overpressures and fluid flow in the Qikou Depression of the Bohai bay basin, China. J. Geochem. Explor. 106, 77–83. https://doi.org/10.1016/j.gexplo.2009.12.009.

Engle, M.A., Doolan, C.A., Pitman, J.A., Varonka, M.S., Chenault, J., Orem, W.H., McMahon, P.B., Jubb, A.M., 2020. Origin and geochemistry of formation waters from the lower eagle ford group, gulf coast basin, south central Texas. Chem. Geol. 550 https://doi.org/10.1016/j.chemgeo.2020.119754, 119754.

Grasby, S.E., Chen, Z., Dewing, K., 2012. formation water geochemistry of the Sverdrup Basin: implications for hydrocarbon development in the high arctic. Appl. Geochem. 27 (8), 1623–1632. https://doi.org/10.1016/j.apgeochem.2012.04.001.

Grassia, G.S., Mclean, K.M., Philippé, G., John, B., Sheehy, A.J., 1996. A systematic survey for thermophilic fermentative bacteria and archaea in high temperature petroleum reservoirs. FEMS (Fed. Eur. Microbiol. Soc.) Microbiol. Ecol. 21, 47–58. https://doi.org/10.1016/0168-6496(96)00043-8.

Head, I.M., Jones, D.M., Larter, S.R., 2003. Biological activity in the deep subsurface and the origin of heavy oil. Nature 426, 344–352. https://doi.org/10.1038/nature02134.

Hermides, D., Kyriazis, D., Makri, P., Ermidou, A., 2020. Geochemical evolution of the thriassion plain groundwaters, attica, Greece. Environ. Monit. Assess. 192 (9), 561. https://doi.org/10.1007/s10661-020-08491-z.

Hitchon, B., Brulotte, M., 1994. Culling criteria for "standard" formation water analyses. Appl. Geochem. 9, 637–645. https://doi.org/10.1016/0883-2927(94)90024-8.

Huang, Y., Yu, Z., Zhang, A., Jiao, Y., Yang, Y., 2018. Main-controlling factors and hydrocarbon accumulation patterns of the buried-hill reservoirs in the western slope of Shulu sag. Special Oil Gas Reservoirs 25, 60–64 https://doi.org/10. 3969/j. issn. 1006-6535. 2018. 06. 011.

Jiang, Z., Chen, D., Qiu, L., Liang, H., Ma, J., 2007. Source-controlled carbonates in a small Eocene half-graben lake basin (Shulu sag) in central hebei province, north China. Sedimentology 54 (2), 265–292. https://doi.org/10.1111/j.1365-3091.2006.00834.x.

Kuo, L.C., 1994. An experimental study of crude oil alteration in reservoir rocks by water washing. Org. Geochem. 21, 465–479. https://doi.org/10.1016/0146-6380(94)90098-1.

Lafargue, E., Barker, C., 1988. Effect of water washing on crude oil compositions. AAPG (Am. Assoc. Pet. Geol.) Bull. 72, 263–276. https://doi.org/10.1306/703C8C13-1707-11D7-8645000102C1865D.

Larter, S., Huang, H., Adams, J., Bennett, B., Jokanola, O., Oldenburg, T., Jones, M., Head, I., Riediger, C., Fowler, M., 2006. The controls on the composition of biodegraded oils in the deep subsurface: Part II—geological controls on subsurface biodegradation fluxes and constraints on reservoir-fluid property prediction. AAPG (Am. Assoc. Pet. Geol.) Bull. 90, 921–938. https://doi.org/10.1306/01270605130.

Lewan, M.D., 1997. Experiments on the role of water in petroleum formation. Geochem. Cosmochim. Acta 61 (17), 3691–3723. https://doi.org/10.1016/S0016-7037(97)00176-2.

Li, F., Zeng, J., 2017. Characterization of origin and evolution of formation water in buried hill of Jizhong depression, China, using multivariate statistical analysis of geochemical data. Geofluids 1–15. https://doi.org/10.1155/2017/5290686, 2017.

Li, H., Cai, C., 2017. Origin and evolution of formation water from the Ordovician carbonate reservoir in the Tazhong area, Tarim Basin, N.W. China. J. Petrol. Sci. Eng. 148, 103–114. https://doi.org/10.1016/j.petrol.2016.10.016.

Li, M., 2016. Regional geochemistry and fluid flow in the palaeogene aquifers of the gaoyou subbasin in the southern part of north jiangsu basin, China. Acta Geologica Sinica - English Edition 90 (3), 946–955. https://doi.org/10.1111/1755-6724.12736.

Li, Q., You, X., Jiang, Z., Zhao, X., Zhang, R., 2017. A type of continuous petroleum accumulation system in the Shulu sag, Bohai Bay basin, eastern China. AAPG (Am. Assoc. Pet. Geol.) Bull. 101 (11), 1791–1811. https://doi.org/10.1306/01251715073.

Li, Y.-P., Jiang, S.-Y., 2013. Major cation/chlorine ratio and stable chlorine isotopic compositions of sediment interstitial water in the Brazos-Trinity Basin IV from the Gulf of Mexico (IODP 308). J. Asian Earth Sci. 65, 42–50. https://doi.org/10.1016/j.jseaes.2012.10.018.

Liu, N., Qiu, N., Chang, J., Shen, F., Wu, H., Lu, X., Wang, Y., Jiao, Y., Feng, Q., 2017. Hydrocarbon migration and accumulation of the suqiao buried-hill zone in wen'an slope, Jizhong subbasin, bohai Bay Basin, China. Mar. Petrol. Geol. 86, 512–525. https://doi.org/10.1016/j.marpetgeo.2017.05.040.

Lüders, V., Plessen, B., Romer, R.L., Weise, S.M., Banks, D.A., Hoth, P., Dulski, P., Schettler, G., 2010. Chemistry and isotopic composition of rotliegend and upper carboniferous formation waters from the north German basin. Chem. Geol. 276, 198–208. https://doi.org/10.1016/j.chemgeo.2010.06.006.

McCaffrey, M.A., Lazar, B., Holland, H.D., 1987. The evaporation path of seawater and the coprecipitation of Br (super -) and K (super +) with halite. J. Sediment. Res. 57, 928–937 https://doi.org/10.1130/0091-7613(1987)15<879:CAROKM>2.0.CO;2.

Michael, K., Bachu, S., 2002. Origin, chemistry and flow of formation waters in the Mississippian–Jurassic sedimentary succession in the west-central part of the Alberta Basin, Canada. Mar. Petrol. Geol. 19, 289–306. https://doi.org/10.1016/S0264-8172(02)00018-1.

Moore, C.H., Wade, W.J., 2013. Carbonate Reservoirs: Porosity and Diagenesis in a Sequence Stratigraphic Framework. Newnes, pp. 59–61.

Panno, S.V., Hackley, K.C., Locke, R.A., Krapac, I.G., Wimmer, B., Iranmanesh, A., Kelly, W.R., 2013. Formation waters from Cambrian-age strata, Illinois Basin, USA: constraints on their origin and evolution. Geochem. Cosmochim. Acta 122, 184–197. https://doi.org/10.1016/j.gca.2013.08.021.

Peters, K.E., Moldowan, J.M., 1993. The Biomarker Guide: Interpreting Molecular Fossils in Petroleum and Ancient Sediments. Prentice-Hall, New Jersey, p. 363 (Englewood Cliffs).

Rittenhouse, G., 1967. Bromine in oil-field waters and its use in determining possibilities of origin of these waters. AAPG (Am. Assoc. Pet. Geol.) Bull. 51, 2430–2440. https://doi.org/10.1306/5D25C27D-16C1-11D7-8645000102C1865D.

Rogers, J.R., Bennett, P.C., Choi, W.J., 1998. Feldspars as a source of nutrients for microorganisms. Am. Mineral. 83, 1532–1540. https://doi.org/10.2138/am-1998-1114.

Röling, W., Head, I.M., Larter, S.R., 2003. The microbiology of hydrocarbon degradation in subsurface petroleum reservoirs: perspectives and prospects. Res. Microbiol. 154, 321–328. https://doi.org/10.1016/S0923-2508(03)00086-X.

Saller, A.H., Stueber, A.M., 2018. Evolution of formation waters in the Permian Basin, United States: late Permian evaporated seawater to Neogene meteoric water. AAPG (Am. Assoc. Pet. Geol.) Bull. 102 (3), 401–428. https://doi.org/10.1306/0504171612517157.

Sanjuan, B., et al., 2016. Major geochemical characteristics of geothermal brines from the Upper Rhine Graben granitic basement with constraints on temperature and circulation. Chem. Geol. 428, 27–47. https://doi.org/10.1016/j.chemgeo.2016.02.021.

Shelton, J.L., McIntosh, J.C., Warwick, P.D., McCray, J.E., 2016. Impact of formation water geochemistry and crude oil biodegradation on microbial methanogenesis. Org. Geochem. 98, 105–117. https://doi.org/10.1016/j.orggeochem.2016.05.008.

Tardy-Jacquenod, C., Caumette, P., Matheron, R., Lanau, C., Magot, M., 1996. Characterization of sulfate-reducing bacteria isolated from oilfield waters. Can. J. Microbiol. 42, 259–266. https://doi.org/10.1139/m96-038.

Tissot, B.P., Welte, D.H., 1984. Petroleum Formation and Occurrence: a New Approach to Oil and Gas Exploration, second ed. Springer–Verlag, Berlin–Heidelberg. https://doi.org/10.1007/978-3-642-87813-8.

Wang, G., Xue, Y., Wang, D., Shi, S., Grice, K., Greenwood, P.F., 2016. Biodegradation and water washing within a series of petroleum reservoirs of the Panyu Oil Field. Org. Geochem. 96, 65–76. https://doi.org/10.1016/j.orggeochem.2016.03.009.

Worden, R.H., Coleman, M.L., Matray, J.M., 1999. Basin scale evolution of formation waters: a diagenetic and formation water study of the Triassic Chaunoy Formation, Paris Basin. Geochem. Cosmochim. Acta 63 (17), 2513–2528. https://doi.org/10.1016/S0016-7037(99)00121-0.

Xiang, C., Lu, Y., Li, J., 2007. Physical properties and genesis of heavy oil in the northern northwest slope zone of the Songliao Basin, Northeastern China. Acta Geol. Sin. 81, 255–260. https://doi.org/10.1016/S1872-5791(07)60044-X.

Xiang, P., Ji, H., Shi, Y., Du, Y., Chen, P., Weng, Q., Xu, X., Sun, Y., Huang, Y., Zou, S., 2021. Characteristics and formation mechanism of mesogenetic dissolution: a case study of Ordovician carbonate in the western slope of the Shulu Sag, Jizhong Depression, Bohai Bay Basin. J. Petrol. Sci. Eng. 206, 109045. https://doi.org/10.1016/j.petrol.2021.109045.

Xie, X., Fan, Z., Liu, X., Lu, Y., 2006. Geochemistry of formation water and its implication on overpressured fluid flow in the Dongying Depression of the Bohaiwan Basin, China. J. Geochem. Explor. 89, 432–435. https://doi.org/10.1016/j.gexplo.2005.11.026.

Yu, H., Ma, T., Du, Y., Chen, L., 2019. Genesis of formation water in the northern sedimentary basin of South China Sea: clues from hydrochemistry and stable isotopes (D, ^{18}O, ^{37}Cl and ^{81}Br). J. Geochem. Explor. 196, 57–65. https://doi.org/10.1016/j.gexplo.2018.08.005.

Yu, H., Wang, Z., Rezaee, R., Zhang, Y., Nwidee, L.N., Liu, X., Verrall, M., Iglauer, S., 2020. Formation water geochemistry for carbonate reservoirs in Ordos basin, China: implications for hydrocarbon preservation by machine learning. J. Petrol. Sci. Eng. 185, 106673. https://doi.org/10.1016/j.petrol.2019.106673.

Yu, X., Liu, C., Wang, C., Zhao, J.-x., Wang, J., 2021. Origin of geothermal waters from the upper cretaceous to lower Eocene strata of the jiangling basin, south China: constraints by multi-isotopic tracers and water-rock interactions. Appl. Geochem. 124, 104810. https://doi.org/10.1016/j.apgeochem.2020.104810.

Zhou, S., Bai, G., Zhang, L., Yang, W., Zhao, X., Jin, F., Wang, Q., Shi, Y., Li, Z., Wang, Z., Wang, Y., 2021. Identifying oil sources in the wen'an slope of the baxian depression, the bohai bay basin, north China. Mar. Petrol. Geol. 128, 104938. https://doi.org/10.1016/j.marpetgeo.2021.104938.